Budapest University of Technology and Economics
Faculty of Mechanical Engineering
Department of Fluid Mechanics

Development of energy harvesting technology for pump condition monitoring wireless sensors

MASTER'S THESIS

Author:
Kamran Ahmadli

Supervisor:
Dr. Josh Davidson
Research Fellow

Budapest, 2021

Declarations

Declaration of acceptance

This thesis fulfills all formal and content requirements prescribed by the Faculty of Mechanical Engineering of Budapest University of Technology and Economics, as well as it fully complies all tasks specified in the transcript. I consider this thesis as it is suitable for submission for public review and for public presentation.

Done at Budapest, 15.12.2021

Dr. Josh Davidson

Declaration of independent work

I, Ahmadli Kamran, the undersigned, hereby declare that the present thesis work has been prepared by myself without any unauthorized help or assistance such that only the specified sources (references, tools, etc.) were used. All parts taken from other sources word by word or after rephrasing but with identical meaning were unambiguously identified with explicit reference to the sources utilized.

Done at Budapest, 13.12.2021

Kamran Ahmadli

Acknowledgements

First and foremost, I would like to thank my supervisor, Prof. Joshua Patrick Davidson, without whom none of this would have been possible. Thanks for the education, the guidance, the support and the mentorship. It was an honor for me to work under his supervision. I would also like to thank Dr. Jo Hwan Ryul, as well as Mr. Janardhan Jagadish, for the guidance and the opportunities.

Big thanks to Prof. Orujaliyev Akif, who guided me to this point and has always been my person of motivation. Finally, I would like to thank my family without whose support I would not ever make this far, all the love to my family. Thanks to all friends for all the support. In the future I wish to see written and published paper in a sphere of finance and economics by Sabina Orujaliyeva.

Thank You.

Abstract

Nowadays, with the development of technology, we try to avoid wire usage and reduce the size of devices and their power consumption. As power consumption is decreasing due to the development of new devices, this allows us numerous opportunities for monitoring low-powered wireless sensors. Energy harvesting is one of the most effective methods of contributing the power of these sensors. This applied technique allows us to convert lost energy from the process into new energy for a new process. This will reduce the maintenance cost of the sensors and will contribute to the long-term functioning of them. Sensors will be able to operate continuously with no need to replace batteries or use extremely complicated wired systems. Wireless energy harvesting devices also open to us new opportunities from geographical aspects, as it is now easier to provide sensors for pumps that operate on deep-water platforms or marine machines. The author will discuss vibration energy harvesting devices and will show how different types of vibration harvesting devices can be used to capture the mechanical energy parasitically lost to the environment by the operating pumps. Mostly concentrating on piezoelectric energy harvesting devices of various designs and power outputs author will also try to develop a model to obtain an optimal design with optimal power output for sensors.

Keywords: *Energy, Pumps, Energy Harvesting, Energy Harvesting Devices, Vibration Energy Harvesting Devices, Piezoelectric Energy Harvesting Devices*

Contents

Chapter 1

Introduction

1.1 Overview of the thesis and its impact

Data collected from industrial equipment is critical for monitoring an asset's performance as well as its health. An advanced analytic method can be used to post-process the collected data in order to more correctly identify or even forecast the consequences, allowing operators to make more informed decisions. This usually necessitates a larger number of sensors or a faster sample rate, both of which result in higher power consumption. This may have a substantial impact on wireless sensor battery life, which customers desire for retrofit installations.

Various ambient energy sources are easily available in and around the pump system. Vibration, pressure fluctuation, temperature gradient, sunlight, and a revolving body (shaft, bearing etc.) are just a few examples. Many techniques, such as piezo-electrics, thermo-electrics, solar cells, electromagnetic field, and others, can be used to recover this wasted energy. The energy captured can be utilized to charge batteries, allowing wireless sensors to operate for longer periods of time or perhaps indefinitely.

Other energy harvesting methods, such as solar cells and thermo-electrics, are constrained by the necessity for sunlight and heat gradients, respectively. The ubiquitous vibration energy allows for continuous energy gathering to power these wireless sensors, which can be put in inaccessible and hazardous environments. Electrostatic, electromagnetic, and piezoelectric mechanisms are the most often explored techniques for energy scavenging applications. One of the earliest basic models of a vibration energy harvesting system was the spring–mass–damper model, during which the energy wasted in the electrical damper is similar to the electrical energy generated. Numerous researchers have explored a number of methods to collect vibration energy efficiently and successfully. An electrostatic-based energy harvesting system, for example, was built using a variable capacitor, which was shown to improve the related voltage output by orders of magnitude. MEMS technology might be used to build an electrostatic vibration to elec-

trical energy converter, according to a recent presentation. In addition to electrostatic approaches, many electromagnetic methods for power production have been developed, such as miniature prototypes utilizing two and four magnets to generate energy using ambient vibrations. A MEMS-based production approach has also been developed, with a finite element analysis demonstrating that the design is an efficient energy harvesting device [1]. A unique method of up-converting the frequency was developed to get larger power production from the supplied vibrations utilizing electromagnetic power generation in a manner suitable with MEMS scale technology [2], in addition to simple cantilever-based models. Roundy [3] has suggested that the piezoelectric technology is the most efficient method of gathering vibration energy.

Due to technological advancements in the last few decades,of complementary metal–oxide semiconductor CMOS circuitry has shrunk dramatically in size and power consumption, resulting in a massive ongoing research toward energy-harvesting devices (EHDs) for the advancement of wireless sensors and wireless communication nodes for ubiquitous networks [4] [5]. Piezoelectric EHDs have gotten more attention because of their self-contained power generation capability, which means they don't need an external voltage source, high energy density, excellent dynamic responsiveness, and capacity to scavenge energy from the range of 1 to 200 $\mu W/cm^3$ ambient vibration energy sources (as new designs and piezoelectric materials becoming accessible, this energy range may rise in the near future.) [5], [6]. Such power level is suitable for 100 μW of typical power demand, making it perfect for wireless sensors and communication network nodes. A popular form for piezoelectric EHDs is a cantilever with a seismic mass and a sandwich construction. This is because a device constructed this way, functioning in the first bending mode with a smaller stiffness, has a reduced resonant frequency, which can simply be tuned to the target ambient vibration frequency for best power production.

The goal of this thesis is to look into the modelling and design of a piezoelectric vibration-to-electricity converter that may be utilized to power wireless gadgets. The aim is to generate several designs of the harvester device. Create mathematical model and Analytical calculation and perform Numerical simulation for maximum energy or power (density) output of proposed Energy Harvesting system. Implementation of the device to the wireless sensor system and analysis of Computational results and optimal design of final developed product [7] [8].

1.2 Pumps. Energy loss regions and their reasons

In general, two types of pumps are well-known and commonly used. There is two kinds of pumps which are positive displacement pumps and dynamic pumps. This project is about energy harvesting devices and their interactions with sensors (sensor nodes) and their networks, which are primarily used in pipeline or dynamic pumps, which is why centrifugal pumps will be explored mostly. Centrifugal pumps are turbomachines that raise a specific volume flow to a specified pressure level in order to convey liquids. In turbomachines, energy transmission is always dependent on hydrodynamic processes, and all pressure and energy differences are proportional to the square of the circumferential rotor speed. Positive displacement pumps, on the other hand, provide the same volume V_{stroke} at each stroke, regardless of the flow velocity or rotor speed. The flow rate becomes $Q = RotorSpeed * V_{stroke}$, and the pressure rise is purely due to the back pressure exerted.

According to Figure 1.1, a centrifugal pump consists of a casing, a bearing housing, the pump shaft, and an impeller. The liquid to be pushed travels from the suction nozzle to the impeller through the suction nozzle. A motor drives an overhung impeller located on the shaft through a connection. The impeller transmits the energy required to carry the fluid in a circumferential direction and accelerates it. Because the fluid flow follows a curved route, the static pressure rises in line with kinetics. The fluid departing the impeller is decelerated through the volute and subsequent diffuser in order to employ as much kinetic energy as possible at the impeller output to raise the static pressure. The discharge nozzle is formed by the diffuser.

The liquid is prevented from leaking into the environment or the bearing housing by a shaft seal, such as a stuffing box or a mechanical seal (the shaft seal is not represented in Figure 1.1). An inducer may be added to the impeller intake to improve suction performance, as illustrated in Figure 1.1. The majority of applications, however, do not employ an inducer.

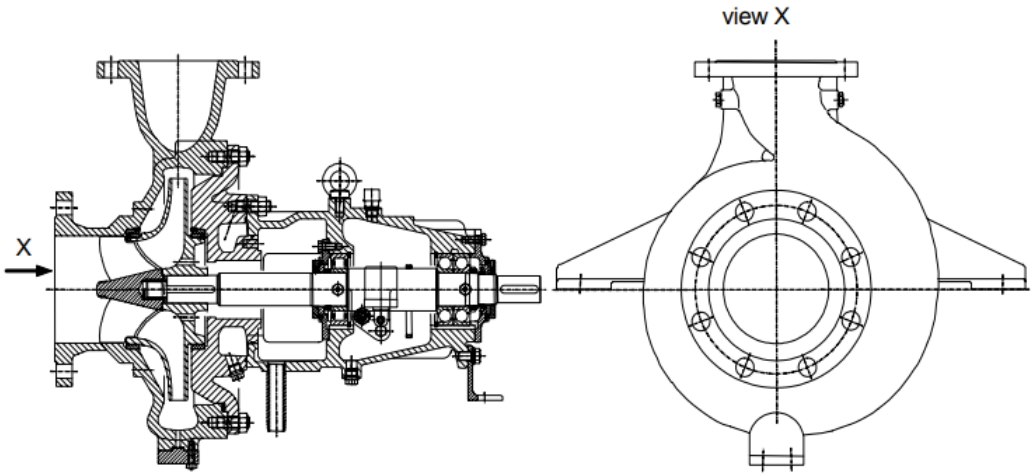

Figure 1.1: Single-stage volute pump with bearing frame, Sulzer Pumps

A small annular seal separates the impeller from the casing, allowing some leakage to flow back from the impeller outlet to the intake. The rear shroud has a second annular seal that counterbalances the axial forces operating on the impeller front and back shrouds. Through "axial thrust balance holes" installed into the rear shroud, the leakage from this seal returns to the suction chamber. The hub, the back shroud, the blades that transmit energy to the fluid, and the front shroud make up the impeller. In other cases, the front shroud is not used. The impeller is described as "semi-open" in this scenario. The meridional section and plan view of an impeller are shown in Figure 1.2. For a given radius, the leading face of the spinning impeller's blade faces the most pressure. It's referred to as the pressure surface or pressure side. The suction surface, or suction side, is the opposing blade surface with the lower pressure. The suction surface is visible while gazing into the impeller eye. As a result, it's also known as the "visible blade face" or "lower blade face," whereas the pressure surface, which isn't visible via the impeller eye, is known as the "upper blade face".

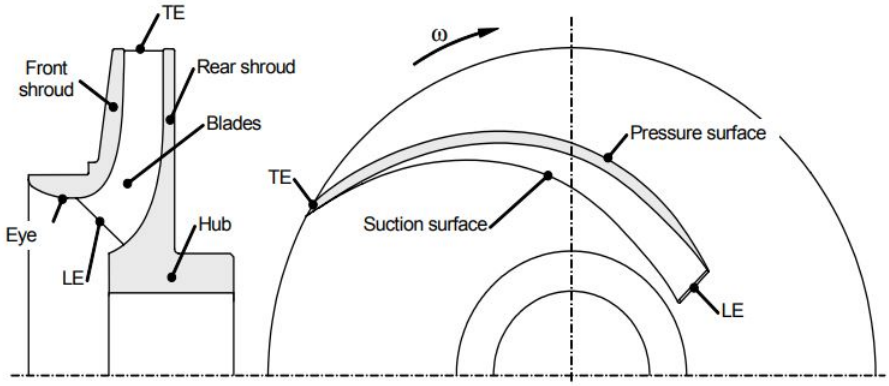

Figure 1.2: Meridional section and plan view of a radial impeller

As it is understandable, mechanical work principle of the centrifugal pump. Physically

this is inevitable to avoid energy losses during the process. Many known mechanical reasons bring to mechanical energy loss of pumps such as vibration of the pump in a time of an operation or overheating of its casing according to rules of fluid viscosity flow through the channel, or the over heating of the rotor shaft and bearings are good example of mechanical energy losses of pumps etc. These are generally known cases of energy losses of the pumps which is nowadays well studied and researched in order to avoid or reduce them. In this thesis project we try convert lost energy into source for another product.

Vibration in Centrifugal pumps: Because vibration has such a big impact on centrifugal pumps' performance, it's important to pay attention to it. Increased vibration levels usually imply a premature failure, which implies the equipment has begun to damage itself. It's because extreme vibrations are the result of a system failure. Excitation factors such as residual rotor imbalance, turbulent liquid flow, pressure pulsations, cavitation, and/or pump attrition are predicted to cause all pumps to vibrate. The quantity of vibration will be increased if the vibration frequency approaches the resonance frequency of a primary pump, foundation, and/or pipe component. Higher vibration levels (amplitudes) are usually symptomatic of mechanical equipment defects developing.

1.2.1 Source of vibration of Centrifugal Pumps

1. Mechanical Causes of Vibrations
    - Bent or warped shafts
    - Rotating components that are unbalanced, damaged Impellers and shaft sleeves that aren't concentric.
    - Thermal expansion of different components, particularly shafts
    - Misalignment of the pump and the driver
    - Strain in the pipes (either by design or because of thermal expansion)
    - Inadequacy or improper construction of foundations
    - Parts rubbing
    - Worn or loose bearings or loose components
    - Defective components
2. Hydraulic Causes of Vibrations
    - Operating pump lower than best efficiency point (BEP)
    - Too close proximity of the impeller vane to the pump cutwater
    - Non-laminar flow of the system (Turbulent flow)
    - Vaporization of fluid

3. Peripheral Causes of Vibrations

    - Vibrations created by nearby equipment or drivers
    - Using a critical speed for the pump
    - Seal faces may seize briefly (if you're pumping a non-lubricating fluid, a gas, or a dry solid via a pump discharge recirculation line aimed at the seal faces).

1.2.2 Sources of thermal losses of Centrifugal Pumps.

Important attention of ours should have the overheating of the pumps which is also lose of considerable amount of energy. As an example, it can be brought that during the operation of the pump as the flow goes through the channel, due to interaction of the fluid with walls of channel as a viscous friction generates heat (the wall heats up) which causes to overheating of casing of the pump. Another example is simply heating of generator rotor shaft or overheating of bearings the reason of which can be inappropriate work of the motor (pump) or lack of lubrication. Aeration - air leaks at seals and fittings on hydraulic system components may let air into the system, causing bubbles to develop in the fluid. When your system compresses air bubbles, they create heat, which is subsequently transferred to the surrounding fluid, warming it. All these examples of heating of pumps are the actual problem that shows either pump does not operate properly else it loses much energy and decreases its durability and life of the system. That is why for proper operation of pumps it is necessary to keep the temperature undercontrol in which case we use thermal sensors. Thermal sensors also can charged with thermal energy harvesting device and be removed from all the wires for convenience which about which it is going to be written and discussed further in this thesis.

1.3 Wireless Sensors and Wireless Sensor Networks (WSN).

Recent research in various scientific fields, including as physics, microelectronics, control, and material science, as well as cooperation between scientists who previously worked in completely different directions, has resulted in the development of Micro-Electro-Mechanical Systems (MEMS). MEMS have succeeded in pushing the boundaries of what was previously thought to be a System-on-a-Chip (SoC). Indeed, MEMS has allowed processors that were previously thought to merely contain logic operations to perceive and even respond to the actual world. Physical parameter measurement and actuation are now feasible thanks to the integration of sensors and actuators into silicon. MEMS aren't the only aspect of the silicon business that has advanced dramatically. RF and digital circuit technologies have also advanced dramatically. Chips are being used to achieve lower-power, higher-frequency transcievers, while digital circuits are shrinking and becoming more densely manufactured. The next step in exploiting the inheritance of this new technology is to collaborate and synergize sensing, processing, communication, and

actuation. Many research teams and corporations are involved in the design and execution of units that contain these four traits because of the opportunities and difficulties given by this area both in theory and in reality. This sort of device is referred to as a "mote" (Node) and may be built as a prototype or as a commercial product. A mote (node) is a self-contained, small sensor unit that can also process and communicate wirelessly. Despite their autonomy, motes (nodes) have a significant advantage in that they may build networks and collaborate according to a variety of models and designs. Wireless sensor networks have been the subject of much study in the fields of communications (protocols, routing, coding, error correction, and so on), electronics (energy efficiency, downsizing), and control (networked control system, theory and applications). It is important how wireless sensors operate and communicate with each other and MCU (MicroControllerUnit). What is wireless network and according to which principles it is built.

1.3.1 Wireless Sensor Nodes

Generally wireless sensors are that type of sensors that do not require any kind of cables or electronic lines. Such devices work on the same principle as wave pulses, with transmitting and receiving on both ends. Generally after collecting data sensor sends it to another closest node that is why this system is called wireless snesor network as many sensor nodes generate as called sensor cloud.

1.3.2 Wireless Sensor Network (WSN)

In a wireless integrated network sensor (WINS) node, you'll find MEMS sensors, RF components, and actuators, as well as CMOS building blocks including interface pads, specialized and general purpose signal processing engines,data fusion circuits, and microcontrollers. To conserve power, more complex but low-duty-cycle applications would be executed in general-purpose processors, while frequently called functions would be done on specialized circuits. The coordinated action over a network of hundreds to tens of thousands of nodes has the potential to have a large-scale influence, thus individual nodes may have limited functionality. Beamforming for improved target identification, multi-hopped communications, the dissemination of time and location information, and coordinated actuation to achieve macro-scale effects from micro-devices are all examples of coordinated activities. Through huge reductions in control and data traffic, the spread of intelligence across the network considerably encourages this scalability. The nodes may include one or more kinds of sensors, are capable of RF communications, and have signal processing engines for both pre-transmission data processing and networking protocol management. The nodes form a self-organizing network and may perform cooperative tasks including beamforming and cooperative communications. Because the nodes must run on tiny batteries or capacitors or harvester device, low-power operation is essential in this application. The challenge then becomes what design decisions must be made in

order for the network to be scalable and operate at low power for an extended period of time. It is shown in the Figure 1.3 for simplification of understadnig how Wireless Sensor Network works.

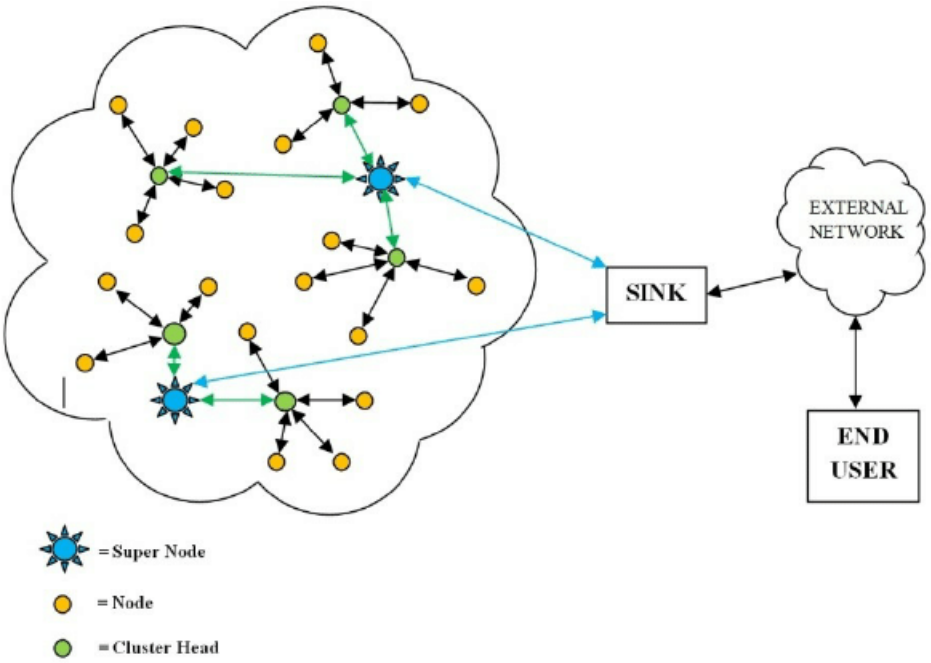

Figure 1.3: General graphic of how Wireless Sensor Network operate

In the Figure 1.3 is shown that as sensors generate cloud (Network) and by sharing between each other data send them to sink (or in other words distributor) that in final delivers data to the user/costumer/company through external network. It Is important to understand how sensors operate in order to design this kind of network. This type of network nodes cannot hold and pass large amount of data that is why we come as dense deployment method. When it comes to low-power RF communications, more signal processing is better than less. The fundamental constraint is that circuits operating at high (RF) frequencies use much more power than circuits operating at low (baseband) frequencies.

As a consequence, even if some additional baseband processing is required, techniques that reduce the quantity of data that should be sent or the power at which it must be supplied result in considerable overall savings. To limit the quantity of data, local decision-making might be employed.This may result in orders of magnitude higher network load savings than merely using data compression. Second, in order to minimize the average transmission power, diversity methods must be used. A dense network of low-cost nodes will permit many transmission pathways. Ground-to-ground communications over long distances suffer from third or fourth power attenuation, which may be mitigated by dense deployment and multi-hopped transmissions. Closed loop power regulation may limit transmission power to the absolute minimum necessary for safe transmission. Even when

the expenses of down and up-conversion of a transceiver relaying messages are included in, this frequently results in a net power savings. More crucially, navigating around barriers such as ridges and slopes will be possible. Frequency variety may also be beneficial in congested surroundings. In the context of fading, diversity approaches allow for power reductions of orders of magnitude. As a result, a more complex radio will use much less power than a radio with limited control flexibility.
There several types of WSN and different applications of theirs such as military applications, environmental, industrial, in robotics or human-centric applications. In this thesis it is important to understand that how these WSN operate in industrial purposes as in this case pipelines and pipeline pumps.

1.3.3 Wireless Sensor or WSN for pump condition monitoring

This project is about design of motion (Vibration) energy harvesting device. As it was discussed that WSN operates with low power supply, and can grant its power from such as batterie, capacitors or in this case from harvester device. In the Figure 1.4 it is shown the whole process and details of how Energy harvester device collaborates with WSN, how the hole system works and how collected data is being transfered to control unit.

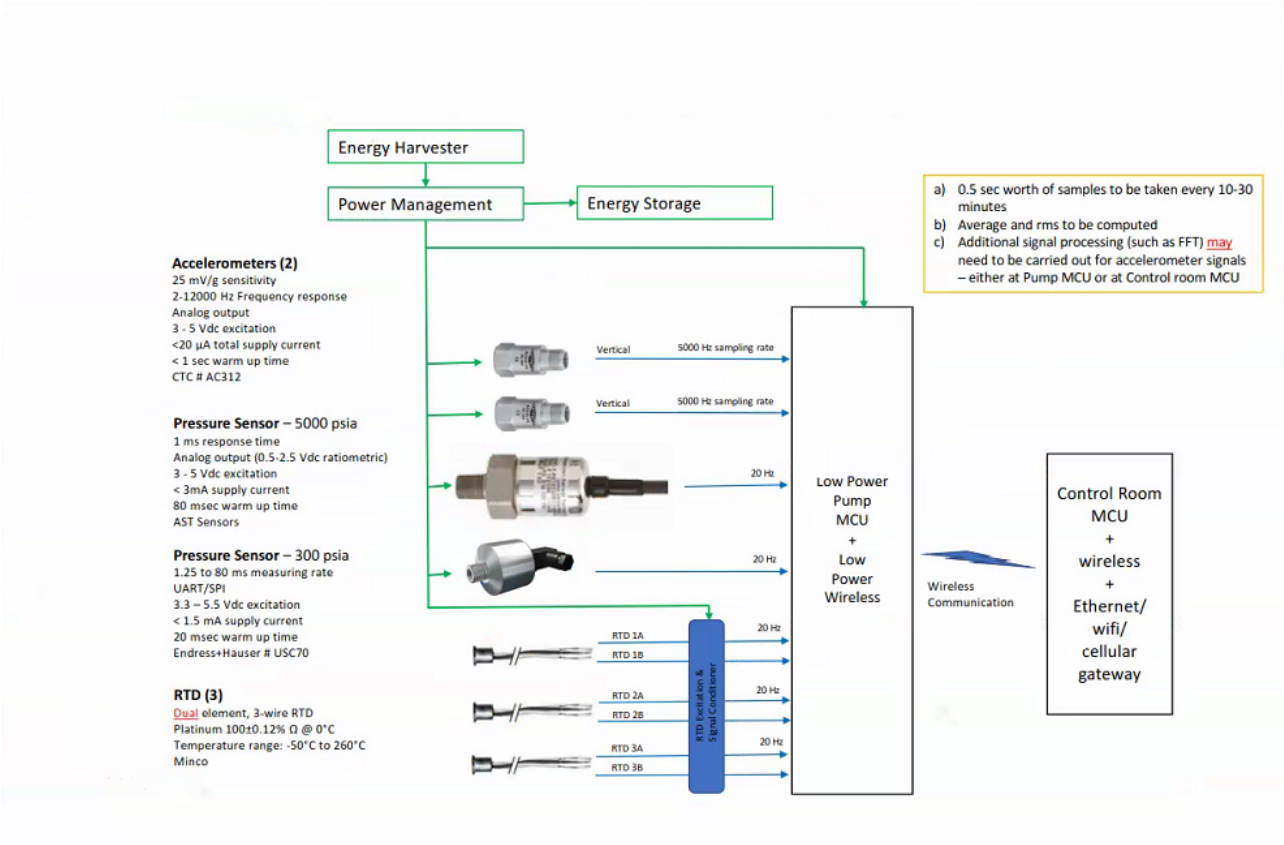

Figure 1.4: Data collection scheme via Wireless Sensor Network powered by Energy Harvester

The working principle of sensors is that the sensor wakes up every hour and collects all the data needed such as Pressure sensors measure 0.5 *sec* worth of pressure data at $20hz$ sampling rate and average, meanwhile accelerometer with sensitivity of $50mV/g$ and frequency response being at 1-9000 Hz collects 1sec worth of vibration data at 2500 Hz sampling rate which perfoms Fast Furier transform and root mean square operation. After all these data collected they are being transfered wirelesly to the microcontroller unit (gateway) which will deliver all the data and information to the customer (company). After all this process done sensors go back to sleep mode and then all this procedure repeats as a loop. Energy harvester device keep working according to its own principle and keep supplying power to existing battery or capacitor of the sensor node.

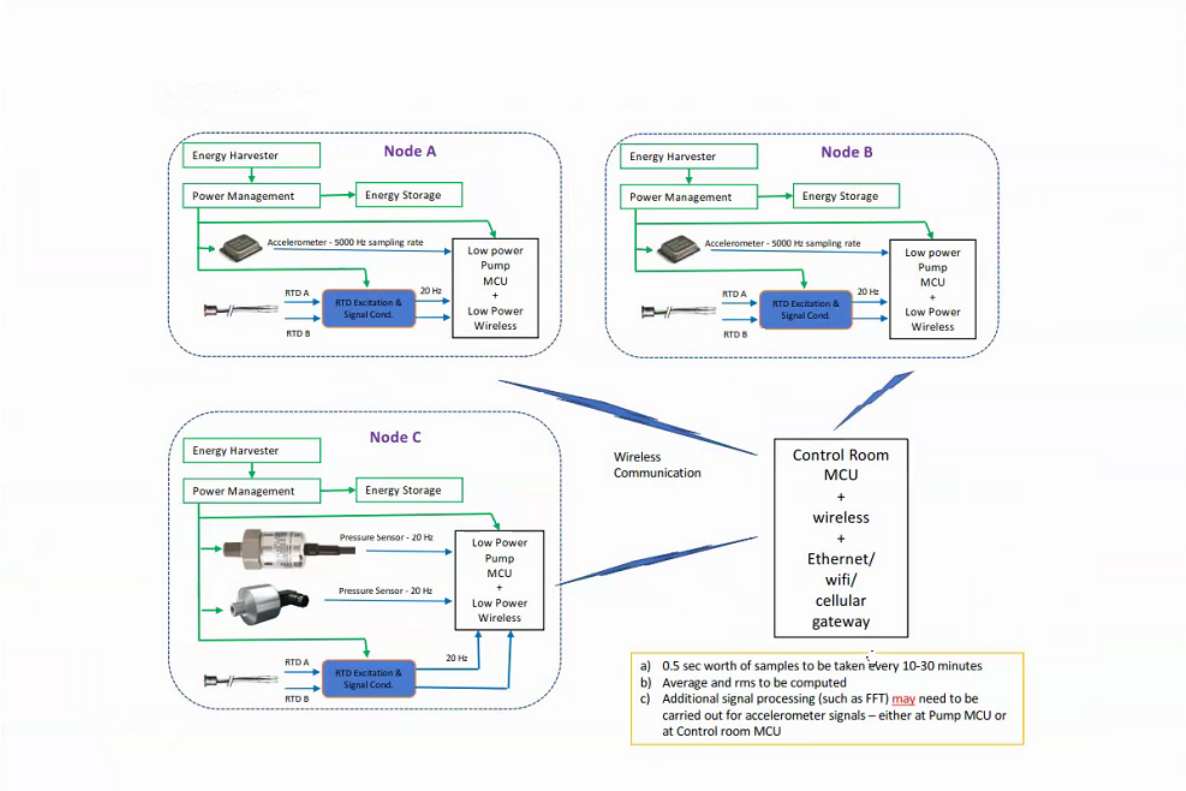

Figure 1.5: Configuration of Wireless Sensors operating individually.

In the Figure 1.5 as an example shown how sensor nodes collect simultaneously and independently collect all the data and transfer it to MCU.

In conclusion, as the thesis research is about energy harvesting devices and their cooperation with sensors, It has been discussed how energy harvester devices become helpful and may be regarded as a revolutionary gadgets that feed power, which is calculated as wasted energy from pumps to the wireless network system, and gathered data by sensors is sent to the control center.

1.3.4 Summary

In this chapter, the general idea of this thesis has been given to outline pipeline-pumps, their association with wireless sensors, and finally choose and design the proper Energy Harvesting Device to power supply the node wireless network. Following this, in this chapter, which types of pumps are overall used, how pumps operate and their construction principles are described. The structure of the pump is a significant part. It further discusses problems that occur during operation and ways to monitor and solve them. The main problem with pumps is energy loss, such as vibration of the pump or overheating of some parts of pipeline pumps, which means that the system does not operate properly. To prevent constant maintenance needs, a better way to monitor the process remotely has been developed. Nowadays, one of the best monitoring methods is wireless network systems, which have been described in this chapter. This is the most efficient and cheapest way to control pipeline pump operations.

In the next chapters, different types of Energy Harvesting Devices will be described in detail. A comprehensive analysis of different types of harvesters and storage units will be discussed. A proper device will be chosen due to the method of application. And in the future, this device will be modeled, designed, and analysed.

The general idea of how the entire system of pump monitoring via WSNs works will be described. The collaboration of harvesters and those sensor nodes, and all the advantages and risks of the development of such a system, will be described.

Chapter 2

Energy Harvesting

2.1 Introduction to Energy Harvesting

Energy harvesting (also known as power harvesting, energy scavenging, or ambient power) for small, wireless autonomous devices such as wearable electronics and wireless sensor networks is the process of capturing and storing energy from external sources (e.g., solar power, thermal energy, wind energy, salinity gradients, and kinetic energy, also known as ambient energy). Energy harvesting is a method of gathering ambient energy and transferring it to suitable for a process energy type. Energy harvesting technique is called a young section of science and researches as it is nowadays so popular with low powered wireless networks. Researchers put more effort into this field of study. An energy harvesting technique is a perfect option for low-powered technologies that have many advantages. For example, low-cost, continuous energy gathering, suitable for places that are hard to reach for maintenance (geographical advantage), can be developed eventually and minimized to a convenient size for used technology, making it the best energy supply technology for sensor networks nowadays. A sensor network is a collection of collaborating embedded devices (sensor nodes) that can recognize and collect data for application-specific evaluation.

Sensing modality, sensor node information processing, communication, and storage capacities, cost and size of every node, type of power source, deployment architecture, data dissemination and communication protocols, applications, and management tools are just a few of the design dimensions of a sensor network implementation. Battery-powered sensor nodes are a common and extensively deployed application type. Industrial machinery monitoring, structural monitoring, vehicle tracking, oil-industry logistics, and alternative energy are some examples of such uses. Untethered sensor nodes employed in these installations allow for greater mobility and deployment in difficult-to-reach regions.

Many techniques were suggested for the best results of the operation of sensors in the battery. Some of the papers relied on changes in types of batteries, increase in size, or use of some other material (type of battery). In all cases, it has been researched for the

purpose of a long life battery so that sensors could operate longer without the need for necessary maintenance or interaction from humans[9] [10] [11] [12]. As a new technique of gathering (harvesitng) energy to supply sensors with it continuously, it revolutionized sensor node network systems. As now, the infinite life-span of networks is no longer a problem, as it reduces the cost of the whole system and relies on itself (no human interaction needed).

Many different types of energy harvesting devices are now in research, developement and in use. They are divided according to harvesting of energy techniques (types of harvesting—for example, sunlight, thermal gradient difference, motion, etc.) and mechanism of convesation ofharvested energy from a source to sensor's rechargable battery. The energy source, the harvesting design, and the load are the three components of a conventional energy harvesting system. The word "energy source" refers to the energy that will be derived from the natural environment. The harvesting architecture consists of technologies that absorb and convert ambient energy into electrical energy. Load is an energy-consuming activity that also serves as a drain for the collected energy.

2.1.1 Energy Harvesting Architecture

Generally, energy harvesting is divided into two architectures: the first is the so-called harvest-use, in which energy is used simultaneously as it is being harvested, second one is called harvest-store-use, in which energy is being harvested whenever it is possible and stored for future use [13]. 1) Harvest-Use Architecture: The Harvest-Use architecture is depicted in Figure 2.1a. Because the sensor node is primarily powered by the harvesting system in this circumstance, the harvesting system's power output must be consistently above the minimal operating point for the node to work. If there is insufficient energy, the node will be disabled. The sensor node will bounce between ON and OFF states if the harvesting capacity changes abruptly at the lowest power point. This is why this kind of architechture is not stable. Harvest-Store-Use Architecture: The Harvest-Store-Use architecture is depicted in Figure 2.1b. The architecture includes a storage component that stores gathered energy while also powering the sensor node. When the gathered energy available exceeds the present demand, energy storage becomes useful. Alternatively, energy can be stored in storage until enough is collected to power the system. If a harvesting opportunity is not available or the sensor node's energy use has to be raised to enhance capacity and efficiency metrics, energy is stored for later use. Secondary storage is used as a backup storage option when primary storage is emptied [14].

2.1.2 Sources of harvestable energy

There is no single source of energy that is perfect for all purposes. The choice is determined by the needs and limits of each application. There are several sources of energy to be

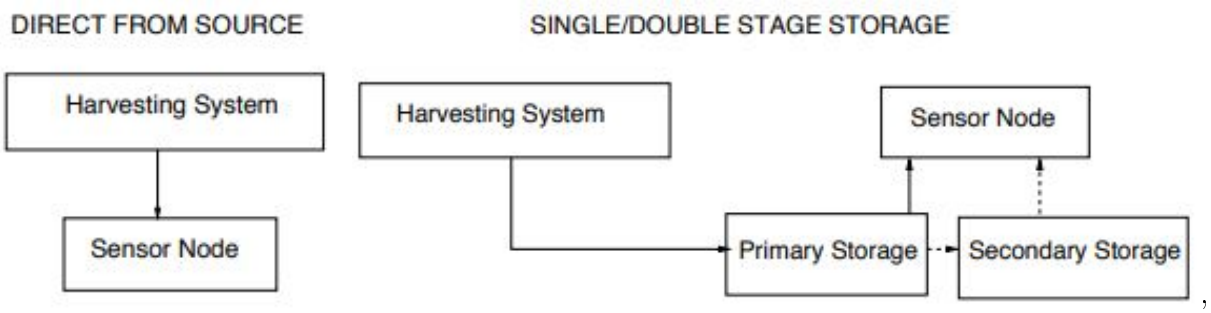

(a) Harvest-Use (b) Harvest-Store-Use

Figure 2.1: Energy Harvesting Architecture

harvested, such as solar, thermal, motion, radio frequencies etc. In the sections that follow, various types of energy harvesting devices that gather energy from different sources and use different mechanisms to pass it to sensor node prototypes will be discussed.

2.1.3 Types of Energy Harvesting Devices and their energy conversion mechanisms

In this section, different types of energy harvesting devices will be discussed, most relying on the papers of [15] [13] [16].Sensor networks can overcome their power supply problem by harvesting energy from their surrounding environment, resulting in significantly longer run-times, years rather than months, and potentially cheaper cost and weight. Depending on the location and environment of the sensor node's deployment, there are several potential energy collecting alternatives.

Types of energy harvesting devices:

- Solar Energy Harvester
- Thermal Energy Harvester (Thermal gradient)
- Mechanical or Motion Harvester
  - Fluid flow
  - Pressure Variation
  - Vibration

2.1.3.1 Solar Energy Harvesting Device (Photovoltaic)

The solar cell is a good and simple example of a solar energy harvesting device. The principle of operation of solar cells is shown in Figure 2.2. It is designed as p-n type semiconductor material. The p-n materials are positioned so that they create a p-n diode junction close to the top surface of the solar cell. When photon radiation strikes the solar cell, an electric voltage potential develops between the p and n-type components, generating power and voltage that can be further transferred to a battery or device (sensor node). Despite the fact that solar cells cannot generate much power (a single solar cell typically produces 0.6 V), the main advantage is that solar cells produce a fairly constant DC voltage over a large portion of their operational range.

To prevent the battery from discharging through the solar cell, solar cells can be linked directly to rechargeable batteries using a simple series diode. Because this incredibly simple circuit does not assure that the solar cell is operating at its optimal position, power generation will be less than the maximum achievable. Second, if a more controlled charging profile is used, rechargeable batteries will last longer. Controlling the charging profile and the working point of the solar cell, on the other hand, necessitates more electronics, which consume power. For each unique application, an analysis must be performed to identify which level of power electronics would supply the highest net level of power to the load electronics. Another factor to consider in this analysis is the battery's lifespan. The main disadvantage of solar energy harvesting is that this device depends on light. This is a reason why this device depends so much on installed geography as installers should take into account number of daily hours, installed place that will be affected directly with sunlight etc.

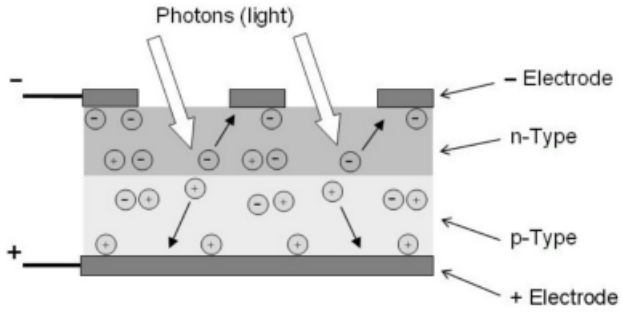

Figure 2.2: Solar cell as a p-n diode [17]

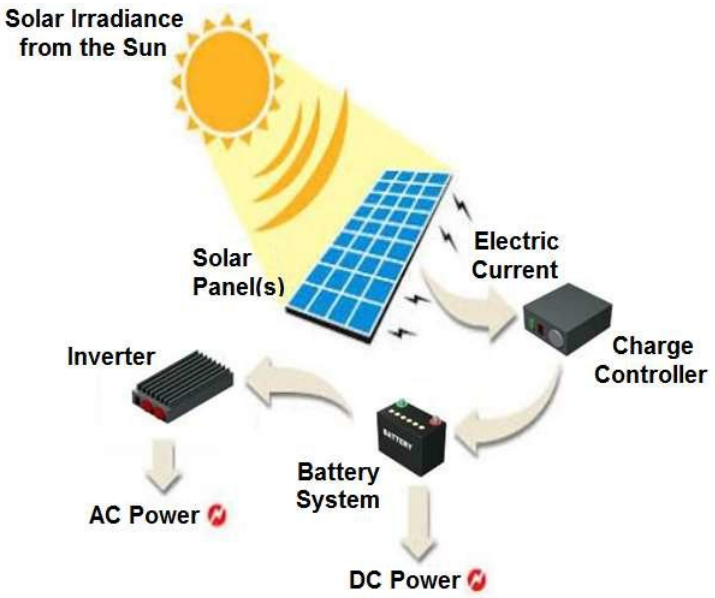

Figure 2.3: Solar energy harvesting configuration

2.1.3.2 Temperature gradient (thermal energy harvesting device)

A temperature difference between two sites causes a flow of heat energy from the hot to the cold location in an attempt to achieve thermal equilibrium. This heat flow can be used to generate useful energy. Because the process is limited by thermodynamic rules, its efficiency, defined as the ratio of useful work extracted, W, to input heat, Q, is constrained by the fundamental Carnot limit. The Carnot efficiency limit is applicable to all heat engines and generators and is represented in terms of hot, TH, and cold, TC, temperature values [18].

$$\nu = \frac{W}{Q} = \frac{T_H - T_C}{T_C} \tag{2.1}$$

Where k - thermal conductivity of the material, A - cross sectional area and Δx - thickness. According to Carnot efficiency, we can assume that if the room temperature is about $20 - 22C^{\circ}$ then the highest temperature of a source is the more efficient we gain.

Assuming heat conduction through silicon material, a good estimate of the maximum amount of power available can be made. Convection and radiation would be insignificant in comparison to conduction at tiny sizes and low temperature differentials. Equation 2.2 calculates the amount of heat flow (power)[16].

$$\dot{Q} = K\frac{\Delta T}{L} \tag{2.2}$$

Where k is the thermal conductivity of the material and L is the length of the material through which the heat is flowing.

According to [16] Thermoelectric technology is a prime use of Thermal Harvesting device. Where temperature variations persist, the thermoelectric effect has the ability to generate electrical energy. Electrons and holes, for example, are free to move and carry both charge and energy. Because the products have a temperature difference, the carriers wander from the hot end to the cold end. The accumulation of charge carriers produces a net charge, which results in the formation of an electrostatic potential within the substance. When the chemical potential for diffusion is balanced with the electrostatic repulsion generated by charge accumulation, the equilibrium condition is obtained. This is the "Seebeck" (Thermoelectric) effect, which underpins thermoelectricity. Thermoelectricity is a physical phenomena that converts heat energy directly into electricity or vice versa depending on the temperature of the object [19].

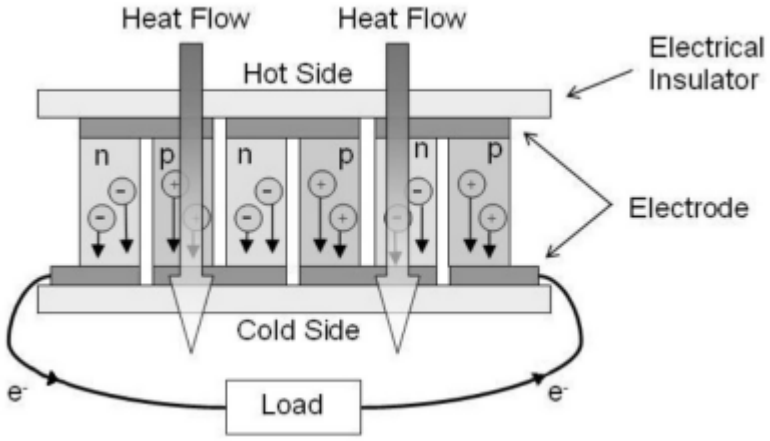

Figure 2.4: Thermoelectric module [15]

The following equation is a relationship beween Temperature difference and induced voltage.

$$V = \int_{T_C}^{T_H} (S_1(T) - S_2(T)dT) \tag{2.3}$$

Where $S_1(T)$ and $S_2(T)$ are Seebeck coffecients which are the functions of temperature, as a result, the voltage across a thermocouple subjected to a temperature differential $T_H - T_L$. Because this voltage is typically fairly low, numerous thermocouples are typically connected in series to form a thermopile in order to generate usable voltages.

2.1.3.3 Mechanical (Motion) Energy Harvesting Devices.

The last topic of Energy Harvesting Devices is about Mechanical Energy Harvesters. This devices are relied on converting available ambient kinetic energy in to electric energy simply using basic physics of motion and energy conservation.

Mostly known Mechanical Harvesters are:

- Fluid Flow
- Pressure Difference
- Vibrations

Fluid Flow

A multitude of methods may be used to convert the flow of any fluid (gas or liquid) to electricity. Wind turbines are becoming increasingly frequent on a larger scale. However, owing to viscosity effects, fresh technologies are necessary at the tiny size for powering sensor networks. For example, a variety of devices based on fluid causing a piezoelectric fin to oscillate owing to vortex shedding have been suggested for usage in both water and air [17].

The output power of a fluid flow is represented by:

$$P = \frac{\rho A v^2}{2} \tag{2.4}$$

Where ρ is being the density of the fluid, A the cross-section area through which fluid flows and v is the velocity of the fluid flow.

Energy-harnessing through fluid-structure interaction has been a hot study field for power supply in the context of ambient energy recovery, with multiple investigations described [20]. Significant research has been conducted on vibration-based aeroelastic energy harvesting using piezoelectric materials, such as flutter-induced vibrations (FIV), vortex-induced vibrations (VIV), and galloping. Flow-induced vibration is a typical phenomena, such as flapping flags and leaves in the wind, flapping water weeds in flowing water, and swing kelp in tides. As a result, researchers have showed a strong interest in collecting energy from flow-induced vibration utilizing piezoelectric materials. FIV and VIV are examples of flow-induced vibration, and fluids include both liquid and air movement. Flow-induced vibration has been shown to be a good excitation method for vibration-based energy harvesting. Both VIV and FIV are fluid elastic instabilities that may generate periodic forces to act on elastic structures, resulting in a coupling of structural and fluid dynamics. Generally, fluid flow harvesting device is best applicable with the research of piezoelectric material for the further purposes of operation. In the Figure 2.5 shown the basic scheme of the VIV with the collaboration of thin piezoelectric layer.

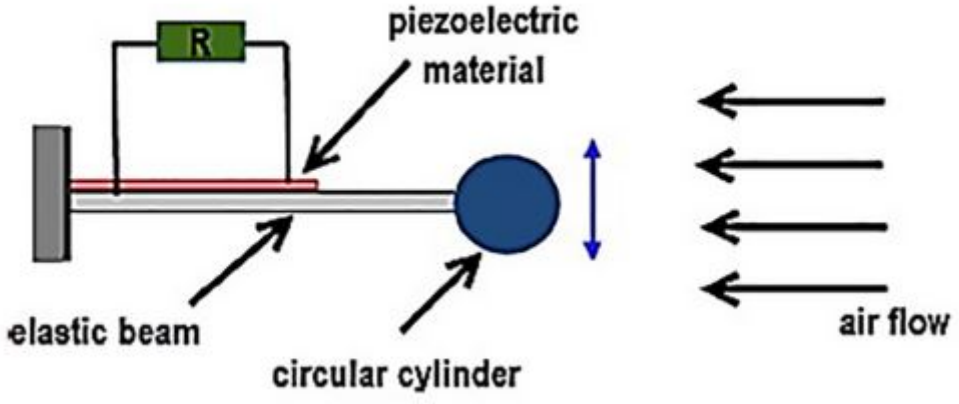

Figure 2.5: Scheme of Piezoelectric Harvester based on VIV [21]

The mechanism of extracting energy from water is analogous to that of air movement. Because maximum power is proportional to fluid density, there is about three orders of magnitude more power available in water for every given volume flowing at a constant speed. Of course, any moving fluid may be harnessed. An oil pipeline, for example, might be a source of fluid energy. Fouling is still an issue with liquid-based fluids, and consideration of the environment is essential prior to the deployment of any sensor network. For the purpose of research it is suggested to research energy harvesting of the fluid flow in the oil pipelines.

Pressure Variation

Application of the Pressure Variation is not very widely researched although in some papers it can be found some theoretical explanation of this kind of harvester devices. Roundy et al. [16] touches and simply explains this topic as a Pressure difference (ΔP) of a fluid in a fixed volume (V) (Constant) which causes Energy change (ΔE).

$$\Delta E = V \Delta P \tag{2.5}$$

Vibration Energy Harvesting Devices

Many other types of energy harvesting devices are available and applicable, however the aim of this thesis relies on research into piezoelectric energy harvesting devices. The overview of mechanical energy harvesting devices will be last.

There are three fundamental processes for converting vibrations to electrical energy: electro-magnetic, electrostatic, and piezoelectric. In the first scenario, the relative motion of a coil with respect to a magnetic field causes current to flow in the coil. Electrostatic generation is made up of two conductors that move relative to one another and are separated by a dielectric (i.e. a capacitor). The energy stored in the capacitor varies as the

conductors move, providing the mechanism for mechanical to electrical energy conversion. Finally, mechanical strain in a piezoelectric material produces a voltage by causing charge separation across the substance (which is a dielectric). These types of Energy Harvester are listed below and will be discussed further.

- Electromagnetic Energy Harvesting Devices
- Electrostatic Energy Harvesting Devices
- Piezoelectric Energy Harvesting Devices

Operation principles of Vibration Energy Harvestig Devices.

Based on linear system theory, one may build a generic model for converting the kinetic energy of a vibrating mass to electrical power without identifying the method by which the conversion occurs. Williams and Yates [4] presented a basic model based on the scheme in Figure 2.5. The following equation describes this system [Equation 2.6].

$$m\ddot{z} + (b_e + b_m)\dot{z} + kz = -m\ddot{y} \tag{2.6}$$

Where z is the spring deflection, y the input displacement, m the mass, b_e and b_m the electrically induced and the mechanical damping coefficients, and k is the spring constant.Following this equation may be derived to more convenient and known form to present resonant frequency. In the [Equation **??**] it is shown the general formula of spring-damping system.

$$\ddot{z} + \frac{b}{m}\dot{x} + \frac{k}{m}x = -m\ddot{y} \tag{2.7}$$

Where we denote $\frac{b}{m}$ as $2\zeta\omega_n$ and $\frac{k}{m}$ as ω.

The main assumption underlying this model is that the conversion of energy from the oscillating mass to electricity (whatever mechanism performs this) appears to the mass spring system as a linear damper. This is a reasonable model for some kinds of electromagnetic converters, such as the one studied by Williams and Yates [4]. This model needs be modified somewhat for various kinds of converters (electrostatic and piezoelectric). For starters, the influence of the electrical system on the mechanical system is not always linear and is not always proportional to velocity. Nonetheless, the conversion will always result in a loss of mechanical kinetic energy, which may be thought of roughly as "damping." Even though it does not precisely simulate certain kinds of converters, its study yields crucial results that may be generalized to electrostatic and piezoelectric systems.

Electromagnetic Energy Harvesting Devices.

Faraday's law of electromagnetic induction is the fundamental concept on which practically all electromagnetic generators are built. Michael Faraday observed in 1831 that

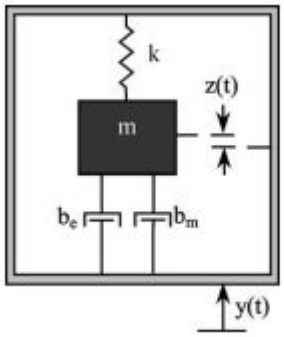

Figure 2.6: General scheme of Mass-Damper system. Generic Vibration converter

moving an electric conductor through a magnetic flux induces a potential difference between the ends of the conductor. Faraday's law states that the voltage, or electromotive force (EMF), produced in a circuit is proportional to the time rate of change of the magnetic flux linkage in that circuit, i.e [22].

$$V = -\frac{\phi}{dt} \tag{2.8}$$

Many electromagnetic inertial microgenerators oscillate at a resonance frequency and may be represented as a second order mass-spring-damper system (which was discussed in subsection 2.1.3.3) made up of a coil connected to a spring and placed in the magnetic field of a permanent magnet. The relative motion caused by the external vibrations between the coil and the magnet produces a voltage at the coil terminals.

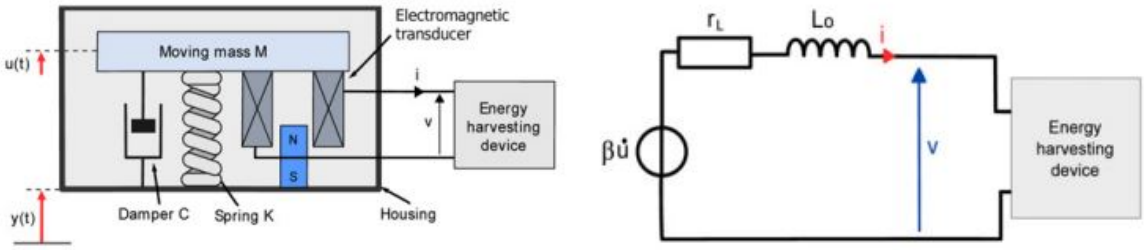

(a) Mechanical model (b) Electrical model

Figure 2.7: An electromagnetic energy harvester model

The energy generated by the generator coil must be transformed into useful electrical energy. An electrical energy extraction circuit does this conversion. Typically, an AC/DC converter is used to rectify the current, and a DC/DC converter is utilized to control the voltage before charging a storage element. A simple and common approach is to examine a linear circuit by substituting the extraction circuit with an equivalent linear input impedance. In this work, this method is referred to as a "classical extraction circuit". This is showin in the Figure 2.7b.

Electrostatic Energy Harvesting Devices.

Meninger and colleagues [23] introduced the first variable capacitor for electrostatic power conversion in 1998. S.Roundy et al. [24] subsequently proved the idea using huge machined variable capacitors. Several variable capacitor architectures for electrostatic harvesting have been documented in the literature since then. The structures of these capacitors are mostly determined by adjusting capacitance characteristics. Variable capacitors are classified into three types: variable area, variable gap, and variable dielectric constant.

S.Roundy et al. [24] have perfectly explained the concept of electrostatic energy harvester and has shown its benefit of being readily incorporated into micro-systems using silicon micromachining and of being capable of increasing energy density with applied voltage, but it does need a separate voltage supplier to "kick-start" it which has some practical issues owing to its complexity. In contradistinction to main concept of three approaches to Electrostatic Harvester S. Roundy and others have shown different proposition explaining another types of such harvesters and devided them like:

(a) In-plane overlap converter

(b) In-plane gap closing converter

(c) Out-of-plane gap closing converter

In the Figure 2.8 are shown all three types.

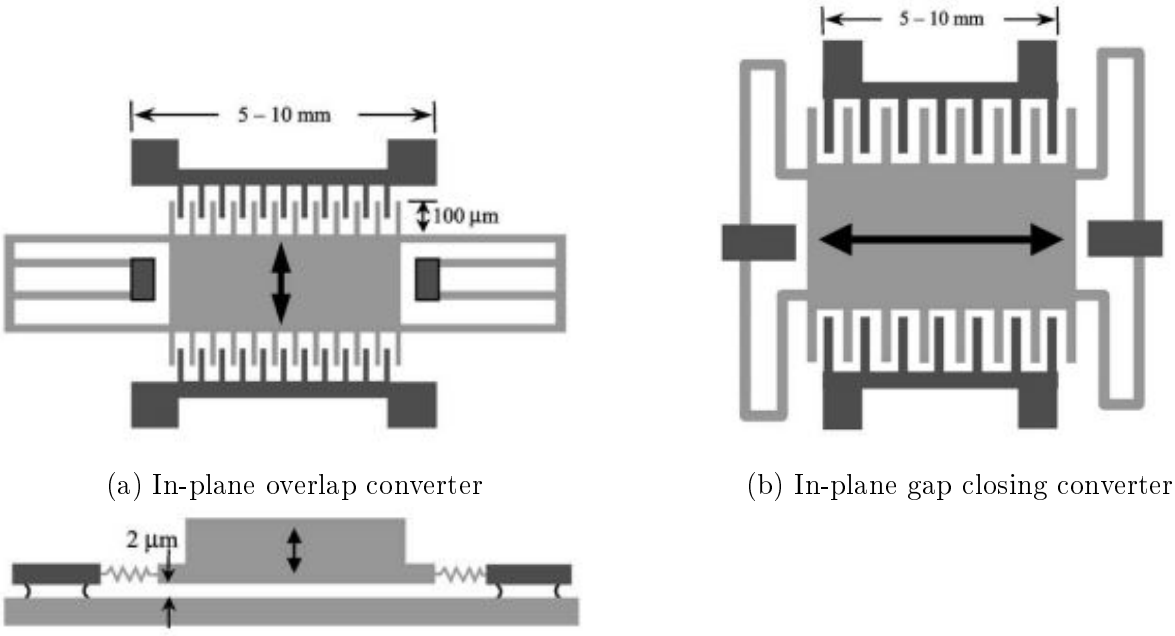

(a) In-plane overlap converter

(b) In-plane gap closing converter

(c) Out-of-plane gap closing converter

Figure 2.8: Electrostatic generators [24]

.

Designing an electrostatic conversion system entails creating a system in which external vibrations vary the gap between two charged capacitive plates kept at constant voltage or constant charge [15]. As the spacing between the plates varies, so does their capacitance, and so energy may be captured as:

$$E = \frac{1}{2}QV^2 = \frac{Q^2}{2C} \tag{2.9}$$

We denote $C = \frac{\epsilon_0 L w}{d}$, where ϵ_0 is a absolute dielectric permittivity of classical vacuum, L and w are the length and width of plates and d is a distance between plates.

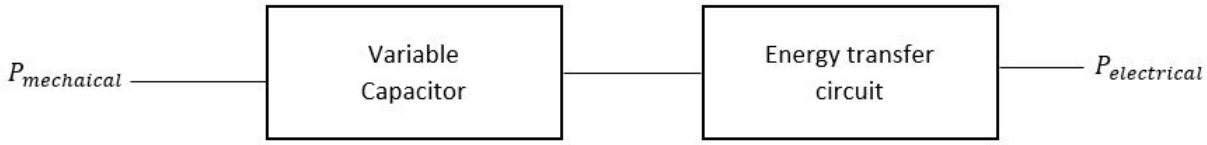

Figure 2.9: Electrostatic Energy Harvesting System.

Electrostatic harvesters are tiny converters with a straightforward design. By modifying the structure of the capacitor, the energy density of these devices may be readily adjusted. By enabling the development of low-cost energy gathering devices, this is a viable answer for increasing the market of energy harvesting powered applications. The structure of the variable capacitor and the conversion mechanism approach are the most important factors in the construction of an electrostatic energy converter. A broad vari-

ety of different structures and methodologies have been offered in research investigations. However, the suggested structures and methodologies offered so far in the literature have both benefits and disadvantages.

The structure of the capacitor is determined by the kind of mechanical energy used: rotational motion or vibration. Kinetic energy may be used to generate both kinds. A variable area capacitor looks to be more suited for capturing rotational energy. The rotating mechanical energy may readily change the area of the capacitor plates. A variable gap capacitor, on the other hand, operates mostly with vibrations. Furthermore, variable area structures can be simply converted into electret-free air capacitors. Capacitance may be increased very easily by increasing the surface area of the capacitor plates.

The variable capacitor structure dictates the conversion technique. The conversion method, as stated in the study, may employ either continuous or switched systems. The continuous method is an electret-based method that necessitates the use of a polarization source and unique manufacturing techniques. While the switched constant voltage and constant charge techniques are less complicated to execute, they nevertheless need switching control circuitry. When the constant voltage and constant charge techniques are compared, it is clear that the former provides more energy. As a result, it is more suitable for electrostatic energy harvesting if it produces low voltages within the breakdown limitations of typical IC manufacturing technologies. The constant charge technique, on the other hand, is appropriate for just a few kinds of electrostatic harvesters, particularly those with high electrostatic forces. The electrostatic force is affected by the capacitor's size, proof mass, and operation conditions. High electrostatic forces are more difficult to create with constant voltage structures than with constant charge structures. As a result, when significant electrostatic forces are needed, continuous charge is preferable.

Piezoelectric Energy Harvesting Devices.

In this section Piezoelectric Energy Harvester (PEH) will be discussed and will be shown the general idea of these devices. How they operate, their advantages and disadvantages briefly will be reviewed. The main concept and operation principles (analytical) of PEH will be shown and explained further in chapter 3.

Piezoelectricity is seen in non-centrosymmetric crystalline materials. This phenomenon produces an electric polarization corresponding to an applied mechanical stress (direct piezoelectric effect) or a mechanical strain proportional to an applied electric field (indirect piezoelectric effect, converse piezoelectric effect). Throughout vibration energy harvesting, piezoelectric materials use the direct piezoelectric effect to turn mechanical strain into an electrical current or voltage. Shortly, when mechanical stress is applied to a piezoelectric material, an open circuit voltage (a charge separation) occurs across

the material. Similarly, when a voltage is applied across a material, mechanical stress (and/or strain, depending on how the material is limited) emerges. The power output of a certain piezoelectric energy harvester is determined by both intrinsic and extrinsic variables. Intrinsic factors include the piezoelectric element's frequency constant, the material's piezoelectric and mechanical characteristics, and the temperature and stress dependency of the physical properties. Extrinsic elements include the input vibration frequency, the acceleration of the base-source structure, and the excitation amplitude. Piezoelectric Harvesters are devided into several piezoelectric harvester setups and characteristics. Variations in the frequency operating range and power output are possible due to the combination of mechanical architecture and material qualities.

Because the piezoelectric material produces its highest power at the electromechanical resonance frequency, the efficiency and power density of a piezoelectric vibration energy harvester are substantially frequency dependant. Because the potential output power is indirectly proportional to the frequency of the fundamental vibration mode, the low frequency fundamental mode should be prioritized in the design of the energy harvesting device. However, since the size and weight limits limit the usage of ceramics to obtain the appropriate fundamental frequency, the design of the energy harvesting structure gets more complicated as the frequency of the vibration base decreases.

The main concept of this Thesis project is to develop optimal design of cantilever type of energy harvester (Figure 2.10). Because a substantial mechanical strain may be created inside the piezoelectric material during vibration, cantilever geometry is one of the most extensively utilized structures in piezoelectric energy harvesters, particularly for mechanical energy harvesting from vibrations. Furthermore, the production of piezoelectric cantilevers is straightforward and affordable. More crucially, the basic bending mode of a cantilever is substantially lower than the piezoelectric element's other vibration modes. The preponderance of of PEH devices created use a cantilever design with a unimorph (one layer of piezoelectric material bonded to a non-piezoelectric layer) or bimorph (two layers of piezoelectric material connected to a non-piezoelectric layer). Because the bimorph structure doubles the energy output without increasing the device volume much, bimorph piezoelectric cantilevers are more widely utilized in piezoelectric energy harvesting investigations than unimorphs. A proof mass may be connected to the free end of the cantilever to further reduce the resonance frequency. It has been discovered that the power output of a cantilever energy harvester is proportional to the proof mass. A zigzag cantilever with a reduced stiffness may also be employed to reduce the structure's resonance frequency.

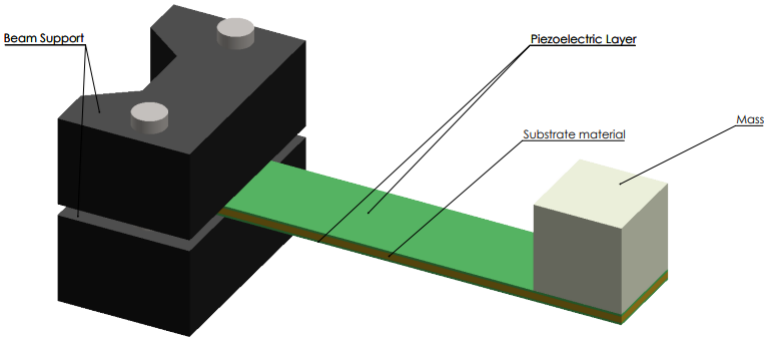

Figure 2.10: Basic concept model of Bimorph cantilever beam Piezoelectric Energy Harvester.

The largest issue in vibration piezoelectric energy harvesting from the standpoint of device design is the mechanical energy sources' low input frequency and acceleration. The majority of VEH are designed to function in resonance mode, with a modest half-power bandwidth. Combining such a low frequency and acceleration for a piezoelectric harvester design becomes difficult as a consequence. Because of this, I and many researcher suffered from design missmatches which cause to lower the power output. As a result, the frequency of ambient oscillations fluctuates widely this field faces challenges. We can observe the most optimal output power while operating around resonant frequency (ω_n). Furthermore, the present level of performance of piezoelectric materials makes constructing an energy harvester that can really replace batteries as a significant power source difficult. The future of piezoelectric energy harvesting is anticipated to be reliant on continual reductions in the energy consumption of electronic devices as well as the development / improvement of the performance of piezoelectric materials utilized in energy harvesting applications.

The major benefits of piezoelectric energy harvesting techniques over electromagnetic and electrostatic approaches are better power density and more flexibility in being incorporated into a single system. The classic piezoelectric energy harvester, consisting of a cantilever beam with piezoelectric devices connected towards its clamped end, is commonly examined and constructed due to its simple construction and simplicity of producing relatively high average strain for a given force input. This simple design with high efficiency brings Piezoelectric Energy Harvesters up on the research and further developments. Which will be discussed further.

2.2 Types of Energy Storage Technologies.

Storage of a gathered energy is an important part of Energy Harvesting Device system. Because wireless sensor nodes have relatively short duty cycles, energy density and cycle life requirements take precedence over power density. Thin-film batteries have showed promise over the last decade and are on the verge of widespread commercialization, but technical challenges such as low capacity per area and high processing temperatures remain. Although thick-film methods will increase capacity, a suitable, practical solid-polymer electrolyte has yet to be widely implemented. While liquid-phase electrolytes are a viable alternative for wireless sensor nodes, the associated packaging costs and environmental constraints are often prohibitive when nodes approach 1 cm^3 or less. Energy is stored in a variety of ways, including electrical charge and hydrocarbon-based fuels. Energy storage cannot provide energy eternally since the stored energy will be consumed and must be replenished at some point. The average energy density, Joules per unit volume, is the statistic used to compare these devices. The following sections describe several energy storage strategies.

Batteries - Microbatteries

Batteries are one option for accumulating charge and storing energy from harvesting and scavenging devices. Because many harvesting systems absorb low quantities of ambient energy, relatively tiny batteries are needed for energy storage and intermittent consumption. Self-powered wireless sensors and wearable electronics are two examples of specific uses. Although standard measures for power, energy, and capacity are milliwatt (mW), milliwatt-hour (mWh), and milliamp-hour (mAh), very tiny batteries are frequently referred to as microbatteries.

There are two kinds of batteries classified: primary and secondary. Primary batteries cannot be recharged with energy, however secondary batteries may reverse their internal chemical reaction during the charging process. This procedure includes delivering energy back into the battery and storing it in the form of chemical bonds. When employing main batteries, the sensor node's lifespan is limited by the set quantity of energy originally stored in the battery. The amount of energy that can be stored in a battery is determined by its energy density and volume. Unfortunately, advancements in battery energy density seem to be hitting a halt. This, along with the need to reduce the volume of every sensor node component, implies that batteries force a significant trade-off between the node's lifespan and its volume.

Secondary batteries, by virtue of their ability to be recharged, give the possibility of prolonging the sensor node's lifespan in comparison to that of a primary battery. This, however, implies that they must be used in combination with another device capable of delivering electricity. This configuration is typically preferable since the component de-

livering power often does so irregularly. The battery retains these bursts of energy, giving a steady continuous energy interface to the electronics. A robust system will need the use of electronics to manage the charging and discharging of the battery in a manner that optimizes its life, since improper charging profiles reduce the battery's useable life [15] [17].

The manufacturer specifies the capacity of a battery, which is done via the use of particular discharge rates. Each producer may choose from a variety of methodologies, which there are several. For non-rechargeable batteries, as an example based on `http://data.energizer.com` the following is used: The discharge rate is set at 25 mA until the voltage reaches 0.8 V. The time taken in hours is then multiplied by the discharge rate (25 mA) to get the milliamper-hour (mAh) capacity. At 0.8 V, a non-rechargeable alkaline battery has practically reached the end of its useful life. It still has a considerable amount of 'overhead' energy, but it can not be utilized. This energy is essentially squandered when the battery is discarded. This is not true with rechargeable batteries, which may be recharged hundreds of times. A similar process is used by a manufacturer to obtain the rated capacity of rechargeable batteries. Their capabilities are based on a 0.1 capacity charge and a 0.2 capacity discharge. So, a rechargeable battery with a capacity of 1,000 mAh will only have that capacity if it is charged at a maximum of 100 mA (for 10 hours) and subsequently discharged at 200 mA. (for 5 hours) [15].

Secondary batteries, like main batteries, have a broad range of properties that are defined by their internal chemistries. Conventional chemistries, such as nickel-zinc (NiZn), nickel metal hydride (NiMH), and nickel-cadmium (NiCd), have high energy densities and excellent discharge rates, but have limited cycle life and negative "memory" effects. These disadvantages are solved by lithium-ion batteries, which have a greater energy density and discharge rate, a higher cell voltage, a longer cycle life, and no "memory" effects . Their main downside is the special care that must be taken during recharging to prevent overheating and irreparable damage. Figure 2.11 depicts the relative strengths of several battery chemistries in terms of energy and power densities.

Micro-batteries and flexible batteries are two potential new areas of study in battery technology. Micro-batteries aim to lower the size of the physical battery while simultaneously improving integration with the electronics they power. As a result, the purpose of micro-batteries is to create a battery on a chip. Overcoming tiny power outputs owing to surface area constraints of micro-batteries is a serious hurdle, but research into three-dimensional surfaces seems promising. The second area entails a new generation of lightweight, flexible batteries [25] that can be molded to any form. As a result, they may serve a dual role of serving as structural material while also lowering the overall volume of the sensor node [22].

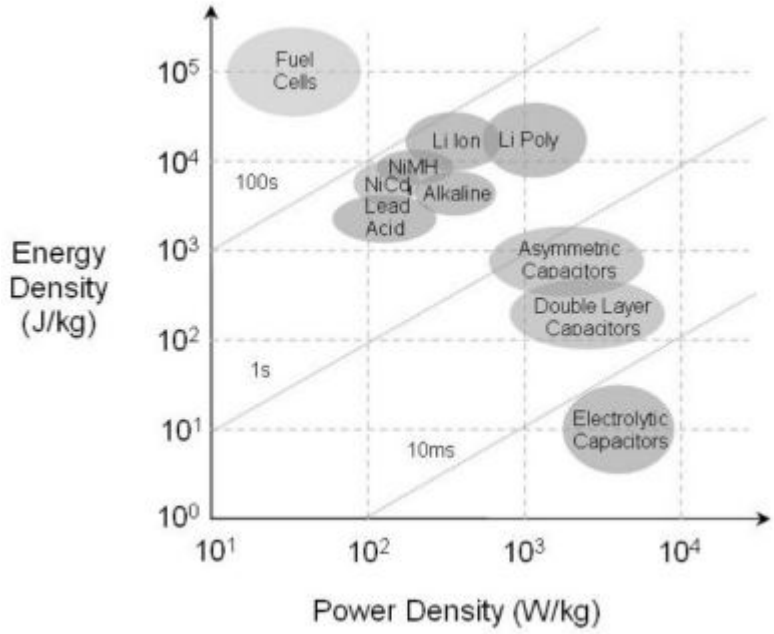

Figure 2.11: Ragone plot for different energy storage mechanisms [15]

Capacitors

The physical shape and structure of practical capacitors varies greatly, and there are many different kinds of capacitors in use. Most capacitors include at least two electrical conductors, which are often in the form of metallic plates or surfaces separated by a dielectric material. A conductor might be a foil, a thin film, a metal sintered bead, or an electrolyte. The nonconducting dielectric works to improve the charge capacity of the capacitor. Glass, ceramic, plastic film, paper, mica, air, and oxide layers are all typical dielectric materials. Capacitors are frequently employed as components of electrical circuits in a broad range of everyday electrical devices. An ideal capacitor, unlike a resistor, does not waste energy, yet real-world capacitors do (see Non-ideal behavior). When an electric potential difference (a voltage) is implemented across the terminals of a capacitor, such as when a capacitor is connected across a battery, an electric field develops across the dielectric, causing a net positive charge to accumulate on one plate and a net negative charge to accumulate on the other. There is no current flowing through the dielectric. However, there is a charge flow across the source circuit. If the state is maintained for a long enough period of time, the current via the source circuit stops. When a time-varying voltage is put across the capacitor's leads, the source experiences a continuing current owing to the capacitor's charging and discharging cycles.

Capacitors have a far better power density than batteries because they can charge and discharge in much shorter periods of time. Their energy density, however, is two to three orders of magnitude lower. Capacitors are thus suitable for giving brief bursts of high power with short operating cycles, enabling the capacitor to recharge until the next burst of power is required. As a result, a capacitor and battery combination might provide the

power needs throughout a typical nodal duty cycle. A battery can meet the low power needs of sleep and receive mode, whereas a capacitor can provide the high power requirements of RF transmission on short duty cycles.

A supercapacitor, like all other capacitors, electrostatically accumulates potential energy. This is what enables the capacitor to provide and absorb a charge quickly while also tolerating exponentially more charge cycles. There is no chemical reaction; nonetheless, supercapacitors vary from regular capacitors in that they use electrostatic double-layer capacitance (EDLC) and electrochemical pseudo-capacitance technology instead of a traditional dielectric between charged plates.

The goal of ongoing research is to boost the energy density of capacitors using a new breed of supercapacitors. A charged supercapacitor is seen in Figure 2.12. The surface area provided by the electrode and the thickness of the double layer created at the electrode electrolyte interface are the essential differences between a supercapacitor and a conventional capacitor. The area of a typical capacitor is just the surface area of a nominally flat plate. The use of porous materials, such as carbon, on the other hand, significantly increases the surface area of each electrode. This enables capacitors with values on the order of 2000 Farads to be housed in packaging similar to ordinary battery sizes [17].

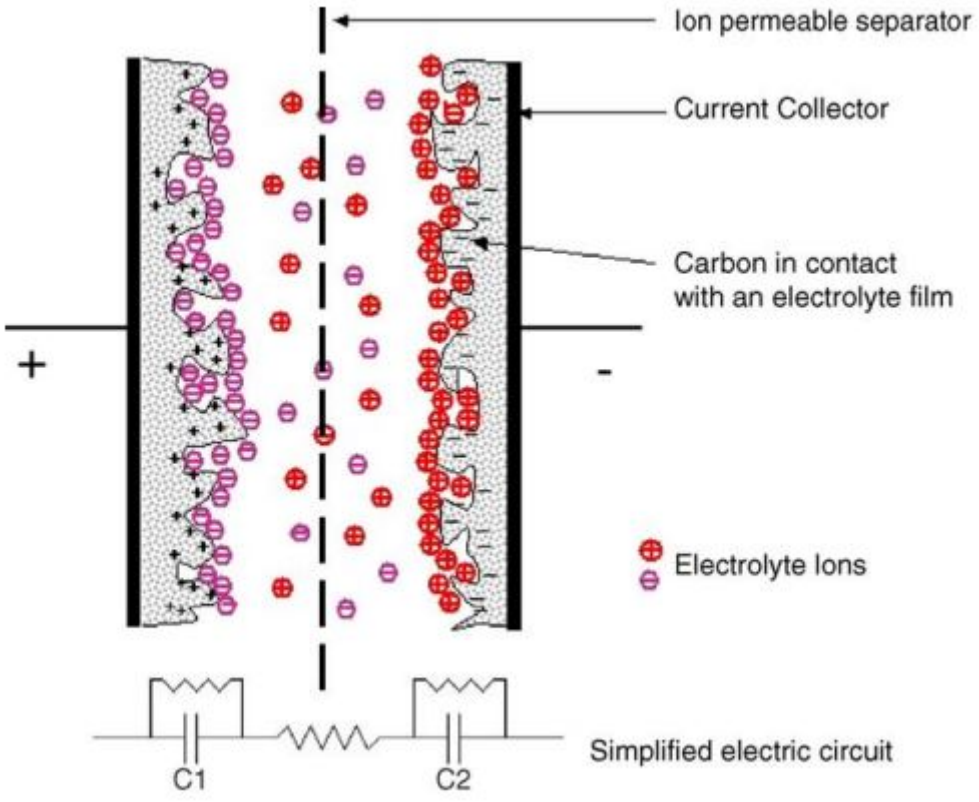

Figure 2.12: Charged Electrostatic Double-Layer Capacitor (EDLC [26]

There are two electrodes in EDLC, a membrane separator and an electrolyte that serves as the dielectric. When a voltage is applied, ion absorption takes place on the surface of each electrode, resulting in charge separation on the order of a few angstorm (0.3-0.8 nanometers). The Helmholtz double layer at the surface of the asymmetrical electrodes stores capacitance.

In a Figure 2.12 is shown short circuit with series capacitors, which denotes us in a sum a total capacitance called cell capacitance C_{cell}. In case of super Capacitors, C_1 and C_2 would be much larger which will decrease twice the size of C_{cell} [26]. As a result, asymmetric capacitors have been developed. An asymmetric supercapacitor is often made up of a battery electrode (commonly a faradaic or intercalating metal oxide) and an electrochemical capacitor electrode (high surface area carbon). In this configuration, the carbon electrode has a substantially higher capacity than the battery electrode. As a consequence, C_cell reaches the capacitance of the carbon electrode alone, resulting in much more energy storage capabilities than a similar symmetric carbon-based supercapacitor. This has resulted in the fabrication of cells with capacitance values exceeding 8,000 Farads.

To conclude this section with comparison of Batteries and Capacitors (Supercapacitors). Batteries and supercapacitors have traditionally worked in tandem. The supercapacitor efficiently transmitted energy, while the rechargeable battery's storage capacity met the demands of a power bank. The gadgets seemed to be unparalleled in their domains. The supercapacitor provided unrivaled power density, while the battery provided outstanding energy density. Recently, improved supercapacitors that break through that barrier have hit the market.
Performance metrics have long been used to evaluate and contrast batteries and supercapacitors. Batteries have a greater breakdown voltage and a higher energy density, however supercapacitors are lighter, have more robust working limitations, a longer life expectancy, and an unequaled power density. The use of nanomaterials is revolutionizing supercapacitors, allowing for larger storage capacity and a wider range of applications. In the realm of energy storage devices in harsh settings, it has now taken on the appearance of a competitive technology to rechargeable batteries. While it remains to be seen how far sophisticated supercapacitors will penetrate the market, rechargeable batteries will remain the go-to technology when higher voltage limitations and more energy density are required and harsh conditions are not a limiting issue.

Other energy storage devices

There are many other energy storage devices such as Fuel cells, thermal storage units etc. which can replace batteries with more power density although with some drawbacks behind them as an installation or efficiency with micro units. These power sources are

well summarized and explained by Dr. J.Davidson [17]. Also as a additional power source great example is Radioactive power source which also has been discussed by Dr. J. Davidson.

Shortly to sum up **Micro fuel cells** are being researched as a replacement for rechargeable batteries, particularly lithium ion batteries. Due to their restricted specific energy, present battery systems are not ideal for high-power and long-life span portable devices, while major research and development is underway to address such limits. Many qualities and factors need be addressed in the development process of tiny fuel cells in order to compete with traditional batteries. The essential qualities are energy, size, weight, operating time, transient behavior, and cost, whereas the related important factors are energy density, specific energy, cartridge for fuel, change of power density with time, specific cost, and life cycle cost. Fuel storage and the fuel cell stack contribute significantly to system volume. Larger levels of fuel storage enhance the system's runtime before needing to be refilled; however, a bigger stack increases the system's overall power and/or efficiency, since tiny fuel cells work more effectively at low power densities. As a result, a bigger fuel cell stack working at lower power densities provides improved efficiency, lowering fuel consumption. As a result, the fuel storage and fuel cell stack sizes should be optimized [27]. The tiny electrode surface area, like with batteries, is the fundamental performance constraint of micro-scale fuel cells. There may be an opportunity to integrate the work of Hart et al. [28] concerning three-dimensional surfaces in battery electrodes with the previously mentioned problems of fuel cell electrodes. Another impediment is the plumbing for the fuel reservoir, which is viewed as a more difficult undertaking at micro-scales than micro-fabricating the electrodes. The key difficulty here is flow concerns and ensuring that fuel flows throughout the cell, especially to the finer tubing at the extremities.

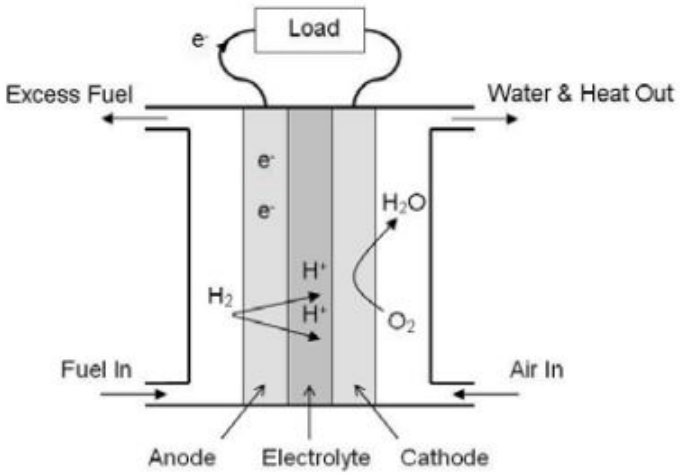

Figure 2.13: Micro-fuel cell unit - polymer electrolyte membrane [15]

2.2.1 Collaboration of Energy Harvesting Devices with wireless sensors(nodes)

All of the major elements, as well as each gadget, have been covered in earlier sections. The whole Energy Harvesting Technology for Wireless Sensor Networks system is separated into three components: Harvester, Storage, and Sensor-Network. When a machine in our condition pump operates, we first gather the ambient energy or lost energy of a pipeline pump, and then the harvested energy is transferred to the storage unit (Rechargeable battery, Supercapacitor, or capacitor). We have to consider the AC-DC current from collected energy, that is why usage of rectifiers is essential in some cases. Finally, whenever the Wireless Sensor is turned "on", it uses the energy from the storage device. After the sensor sends the information to the MCU, the sensor turns "off", and the system continues to run in that basic loop.

Conclusion

In conclusion, every component has been discussed separately for the energy harvesting devices for pump condition monitoring wireless sensors. Although some devices and technologies need more time, development and research, nowadays it is accounted ideal condition usage of Energy Harvesters as there is a minimal demand of a power in micro-units or wireless sensors. When scaled down to nodal sizes, however, their efficiencies become prohibitively modest. The battery is currently the greatest source of energy for short-term usage among the technologies available. Energy harvesting is critical for long-term sensor installations, and there are several ambient energy sources that might be used. The energy harvesting technique used for a specific sensor node will be determined by which of these sources is available in the environment in which it is installed.

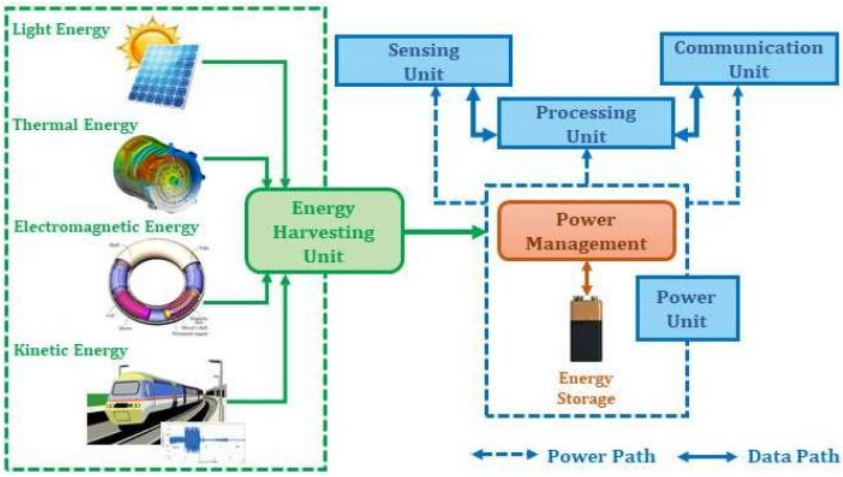

Figure 2.14: Energy Harvesting devices architecture with WSN

2.3 Energy Harvesting Application - Pipeline Pumps

In this section, the implementation of Energy Harvesting devices and the whole system of Wireless Sensor Networks applied to the pipeline pumps will be discussed. The importance of this technology is because of the high demand in this field of industry. Nowadays, the biggest energy production industry is oil, and pipeline pumps are accounted as the most efficient means of transportation for crude oil. It is important to understand that not all pipeline pumps are maintenance-affordable and preservation of such technologies is essential and of high cost (installing traditional devices is exorbitantly expensive). This is a reason to keep pumps under constant control by monitoring them with such a system. This is also a reason to develop such a technology with critical service yet with minimal instrumentation and intelligence. Reducing wires out of sensors enables the implementation of a condition monitoring network on remote equipment at a nominal cost. This technology is found as a new business stream, and this is also one of the important reasons why the field should be invested in, researched and developed.

However, Energy Harvesting technology with Wireless Sensor Networks has many pros, but research and development and implementation of these devices into the industry has their own risks. For example, in this discipline, wireless technology may be not accepted by the industry. The developed technology may not be mature enough to adequately power pump monitoring systems. Another risk is that these devices may lack area certifications for low-powered devices. It is significant to know while designing such a system where it will be implemented from a geographical point of view.

Measurement strategy and design of such technology are discussed with high priority. An evaluation strategy for the design of a mechanism is listed below:

- Sensors and MCU are by default in sleep state
- External/Internal inputs wakes the sensors and MCU
- MCU acquires data from sensors, processes it and then wirelessly transmits to control center
- Operation modes
  - Normal: Wake up every 10 to 30 minutes.
  - Abnormal: Wake up due to sudden changes in pressure or temperatures.

2.4 Summary

The information described in Chapter 2 is a study of a technology that is critical in the design and development of pump condition monitoring through Wireless Sensor Networks, using the power of Energy Harvesting Technology. As the scale of electronic units decreases, this field should be researched and discussed more for the future. A significant aspect of a field is an application. The application field of the harvester devices should also be considered according to the demand curve (plot) for such products. Also, not to mention the geography of use of energy harvesting devices, which is also very weigh detail.

In this chapter, different types of harvesters have been shown and discussed. For the future applications, you can choose them according to the situation and field of operation. It has been shown that different types of storage units can be implemented for the collaboration of harvesters with sensors. In general batteries are optimal storage unit for such a system, however, capacitors also should have our attention. It was suggested for future application to make significant steps in the research of supercapacitors.

It has been described and discussed how wireless sensors communicate with one another and with the control unit. In general, why wireless sensor networks are such revolutionary systems nowadays.

Finally implementation of such a system into pipeline pump condition have been also described. Advantages, risks and disadvantages are the most significant part that should gather customers or engineers attention while ordering or designing such complicated system.

Chapter 3

Vibration Energy Harvesting device on Piezo-Electric material basis

In the previous chapters, it was discussed that this thesis project is focused on the design and development of the Vibration Energy harvesting device that operates on the principle of mechanical energy conversation via piezoelectric material. Many papers and topics were written and many discussions were had in this field. This is obvious because the development of piezo-materials is so popular nowadays, research on these materials is growing, and the scale of power consumption is decreasing to macro sizes because of recent advancements in portable and wearable electronics, wireless electronic systems, implantable medical devices, energy-autonomous systems, monitoring systems, and MEMS/NEMS-based devices. The procedure of small-scale energy generation may usher in a revolution in the development of compact power technologies. That's because the Piezoelectric Energy Harvesting Technology develops with it.

Some drawbacks of PEH (Piezoelectric Energy Harvester) may appear such as high output resistance which causes generating considerably large output voltages at low electrical current. Very sensitive to temperature changes which has been analyzed by Sharma and Baredar [29]. It was analyzed some other disadvantages of PEH. According to them, the shortcomings of piezo-harvesters include depolarization, rapid breaking of the piezo layer owing to high brittleness and weak coupling coefficient, poor adhesive qualities of PVDF material, and lower electromagnetic coupling coefficient of PZT. They explored upcoming difficulties such as the design of high-efficiency energy harvesters, the development of novel energy harvesting designs by researching non-linear advantages, and the design of portable compact-size systems with integrated functionalities.

Taware and Deshmukh [30] conducted a quick assessment of the literature in the topic of piezoelectric energy harvesting. They discussed the benefits and drawbacks of various piezoelectric materials. They discussed cantilever-based piezoelectric energy harvesters, their design considerations, and mathematical modeling.

As for mathematical model of the PEH many papers was reviewed. Batra et al. [31] addressed numerical analysis and structural equations for piezo-materials, distributed parameter modeling, piezoelectric energy conversion methods, and piezoelectric energy harvester working mechanism.

Zhu et al. [32] provided great numerical analysis and increase of power output of PEH using Finite Element Method (FE) simulators and provided FE computation to design Piezoelectric Harvesting Device with optimal design of cantilever beam with approximately output power in a range of 300-400 μW even higher.

For material selection the great review was made by Calio et al [33]. They examined the material characteristics of about 19 piezo-materials, the functioning modes of piezo-harvesters, resonant/non-resonant operations, ideal beam shape, frequency tuning, rotating device topologies, power density and bandwidth, and conditioning circuits. They attempted to give a guide for selecting piezoelectric materials based on power output and operating modes. They came to the conclusion that the resonant d_{33} cantilever beam has to be tuned, and the d_{15} harvester is still too complicated to build despite its immense promise. Here d_{33} and d_{15} strain coefficient for the common piezoelectric material.

Many papers and researches were reviewed, but it has been decided to build a mathematical model of the Piezoelectric Energy Harvester according to Roundy and Wright [34]. The general idea, the design of the cantilever beam and the comparison were made according to this paper and the research of Roundy and Wright. After generating the mathematical model, the vibration data of the pipeline pumps provided by our industrial partners was implemented and has been compared further with experimental methods.

3.1 Mathematical simulation and analysis

Basic mathematical model

The development of the performance of an analytical solution of the generator model is necessary for supposing how much power needed from a possible source of vibration, by doing so the system developer can improve an accurate model. Also, parameters of the geometry can be developed, if the given model will be improved in accordance with an optimization routine. By undertaking these targets, for the piezoelectric generator in Figure 3.1 an analytical model has been optimized.

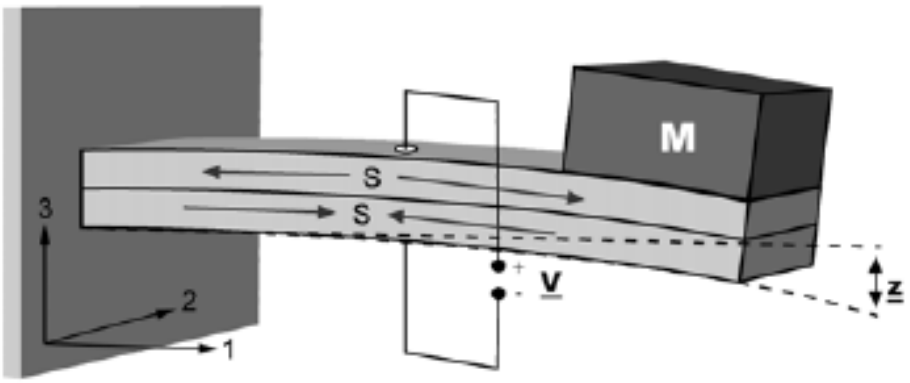

Figure 3.1: A two-layer bender established as a cantilever. Where S is strain, V is voltage, M is mass, and z is vertical displacement. [34]

Following the derivation given in Roundy and Wright [34], he reduced-matrix form for settled fundamental equation of a linear piezoelectric material is given below

$$\{S\} = \left[s^E\right]\{T\} + [d]^t\{E\} \tag{3.1}$$

$$\{D\} = [d]\{T\} + \left[\varepsilon^T\right]\{E\} \tag{3.2}$$

Where $\{S\}$ is the six-dimensional strain vector, $\{T\}$ is the stresses vector, $\{D\}$ is the vector of three-dimensional electric displacement, $\{E\}$ is the vector of electric field ,$\left[s^E\right]$ is at constant electric field evaluated six by six compliance matrix, for piezoelectric strain coefficients $[d]$ is the three by six matrix , and evaluated at constant stress $\left[\varepsilon^T\right]$ is the three by three dielectric constant matrix . The demonstrated nomenclature implemented by Tzou in 1993 (Piezoelectric Shells) are shown here. T denotes the stress caused by a combination of mechanical and electrical factors, while σ denotes the stress caused only by mechanical causes.

In the Figure 3.1 it is assumed that a two-layer bending element established as a cantilever beam. The material is poled along the 3 axes, as is customary for bending elements, and electrodes are mounted on the surfaces are perpendicular to the 3 axes. It is believed that driving vibrations occur exclusively along the three axes. Considering these assumptions, the piezoelectric material is driven in a one-dimensional condition along the 1 axis. The piezoelectric constitutive equations simplify to the formulas in equations (3.3) and (3.4) in this stress condition. It should be noted that plane stress formulations were not explored. Although this may result in minor mistakes, these errors are deemed insignificant given the beam design and size under consideration.

$$S_1 = s_{11}^E T_1 + d_{31} E_3 \tag{3.3}$$

$$D_3 = s_{31}^E T_1 + \varepsilon_3^T E_3 \tag{3.4}$$

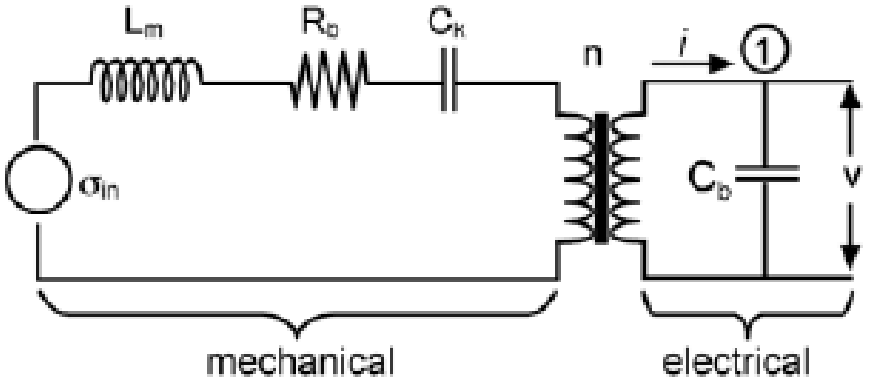

Figure 3.2: The piezoelectric generator's circuit diagram. (Consider that in the formulation of equation (3.5), node 1 is included.) [34]

Following that, D_3, E_3, S_1, T_1, $s_1^E 1$, and ε_3^T can be described such as D, E, s, S, T and ε for the purpose of convenience. Furthermore, the elastic constant,$c = s^1$, will be applied in instead of the compliance, s.

Modeling both the mechanical and electrical components of a piezoelectric network as circuit components is a useful way of modeling piezoelectric elements so that system equations can be readily produced. After that, the electro mechanical interaction is represented as a transformer [35]. Figure 3.2 depicts the bender system's analogous circuit in Figure 3.1. The analogous inductor, L_m, indicates the generator's mass or inertia. Mechanical damping is represented by the corresponding resistor[3],R_b. The mechanical stiffness is represented by the corresponding capacitor, C_k. σ_{in} is an analogous stress generator that describes the stress generated by the source vibrations. The analogous turns ratio of the transformer is represented by n. The the piezoelectric bender's capacity is denoted by C_b . The voltage across the piezoelectric device is denoted by V. From mechanical pint of view of the circuit, the 'across' magnitude is stress, σ (which is equivalent to voltage), after which the 'through' component is strain rate, $\dot{S}$. (equivalent to current).

From the mechanical point, the circuit is considered like a mechanical system which is an uncoupled when using this modeling approach. As a result, the stress variable is σ rather than T, and the stress–strain relationship is $S = s\sigma$(or $\sigma = cS$)). The piezoelectric coupling can be indicated by the transformer. Transformers are distinguished by a turns ratio, which compares voltage on one side to voltage on the other. Stress from the the mechanical behavior is proportional to voltage of the electrical meaning in this scenario.

The equations considered as a system and then derived by Kirchhoff's voltage law (KVL) and Kirchhoff's current law (KCL), as with purely electrical circuits (KCL). The expression in equation (3.5) is obtained by adding the 'voltages' around the mechanical side of the circuit. The expression in equation (3.6) is obtained by adding the currents at node 1 in Figure 3.2.

$$\sigma_{in} = L_m\ddot{S} + R_b\dot{S} + \frac{S}{C_k} + nV \tag{3.5}$$

$$i = C_b\dot{V}. \tag{3.6}$$

Alternative formulations for $\sigma in, Lm, Rb, Ck, n,$ and i must be discovered before these expressions can be turned into a workable system model.

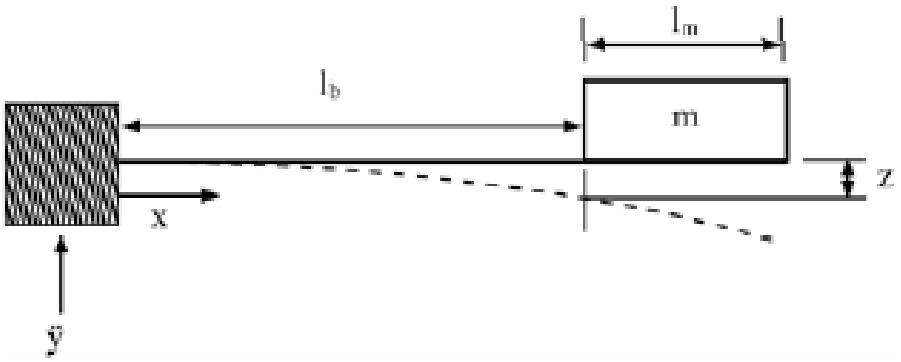

Figure 3.3: The generator's schematic illustration. [34]

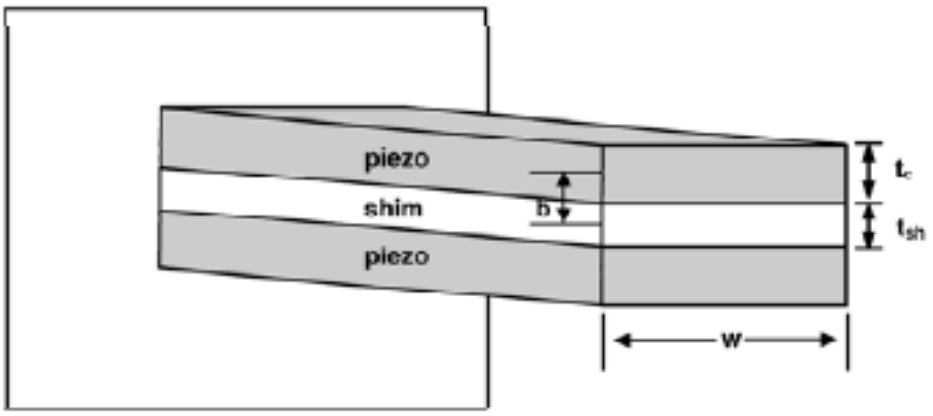

Figure 3.4: The composite beam's schematic illustration. [34]

Figures 3.3 and 3.4 show schematic representations of the converter and composite beam, as well as the geometric parameters. The efficient inertia moment can be required since the piezoelectric bender known as a composite beam. The equation (3.7) below gives the functional moment of inertia.

$$I = 2\left[\frac{\omega t_c^3}{12} + \omega t_p b^2\right] + \frac{\eta_s \omega t_{sh}^3}{12} \tag{3.7}$$

where ω as the beam width, η_s is the center shim's ratio of an elastic constant to piezoelectric material ($\eta_s = c_{sh}/cp$ where c_p is the piezoelectric material elastic constant and

c_{sh} is the center shim elastic constant), and other parameters are as can be seen in Figures 3.3 and 3.4.

The piezoelectric ceramic's elastic constant is then applied in combination with the effective moment of inertia, as demonstrated by equation (7). The term η_s in the moment of inertia accounts for the varied Young's modulus of the center shim [36].

The input stress that can be analogous , σ_{in}, is caused by an input force, F_{in}, which is produced as a consequence of the vibration of an input as from the proof mass , $\ddot{y}$. As a result, σ_{in} may be written as

$$\sigma_{in} = k_1 F_{in} \tag{3.8}$$

Where in the piezoelectric material to the force generated by the mass at the beam's end k_1 is a geometric constant that relates the mean stress. Take into account the formulation of the beam's average stress , σ, as indicated in equation (3.9) to get an expression for k_1.

$$\sigma = \frac{1}{l_e}\int_0^{l_e} \frac{M(x)b}{I}dx \tag{3.9}$$

Where $M(x)$ denotes a moment, l_e is the electrode's length of contacting piezoelectric material. The electrode does not have to carry the entire length of the beam; but, for the purposes of the model provided here, it will be considered that $l_e \leqslant l_b$. To put it another way, the electrode does not reach under the mass. The representation for the moment is provided by

$$M(x) = m(\ddot{y} + \ddot{z})(l_b + \frac{1}{2}l_m - x). \tag{3.10}$$

An expression $m(\ddot{y} + \ddot{z})$ is a composite for the input force, F_{in}, and the force of inertial systems , F_m. Simply replacing $F = F_{in} + F_m = m(\ddot{y} + \ddot{z})$ into equation (3.10), equation (3.10) into equation (3.9), and integrating produces the following interpretation:

$$\sigma = F\frac{b(2l_b + l_m - l_e)}{2I} \tag{3.11}$$

The constant, k_1, is then

$$k_1 = \frac{b(2l_b + l_m - l_e)}{2I} \tag{3.12}$$

Keeping in mind $F_{in} = m\ddot{y}$, the interpretation for σ_{in} turns

$$\sigma_{in} = k_1 m\ddot{y}. \tag{3.13}$$

The inertial force $F_m = m\ddot{z}$ causes the tension across the 'inductive' element in Figure 3.2. The stress caused by inertial effects is then expressed as

$$\sigma_m = k_1 m\ddot{z}. \tag{3.14}$$

Instead of displacement in equation (3.14) , the element's analogous inductance is

L_m, that links stress with strain's time derivative of the second order (note equation (3.5) shown before). An equation connecting average strain, S, to vertical displacement, z, must be derived in order to derive the expression for L_m. Consider the usual beam equation, which is represented in equation (3.15).

$$\frac{d^2z}{dx^2} = \frac{M(x)}{c_pI} \tag{3.15}$$

where I known as the inertia's composite moment that explained using an equation (3.7). When equation (3.10) is substituted for equation (3.15), the result is

$$\frac{d^2z}{dx} = \frac{1}{c_pI}m(\ddot{y}+\ddot{z})(l_b+\frac{1}{2}l_m-x). \tag{3.16}$$

To generate an expression for the deflection term, z, an integration yields

$$z = \frac{m(\ddot{y}+\ddot{z})}{c_pI}\left(\left(l_b+\frac{1}{2}l_m\right)\frac{x^2}{2}-\frac{x^3}{6}\right). \tag{3.17}$$

The formula for z changes at the point where the beam reaches the mass (at $x = l_b$)

$$z = \frac{m(\ddot{y}+\ddot{z})l_b^2}{2c_pI}\left(\frac{2}{3}l_b+\frac{1}{2}l_m\right). \tag{3.18}$$

Regarding substitutions $\sigma = c_pS$ and $m(\ddot{y}+\ddot{z}) = F$ into equation (3.11) above, strain can be represented as follows.

$$S = \frac{m(\ddot{y}+\ddot{z})b}{2c_pI}\left(2l_b+l_m-l_e\right). \tag{3.19}$$

After modifying equation (3.19), the force component, $m(\ddot{y}+\ddot{z})$, may be expressed as indicated in equation (3.20).

$$m(\ddot{y}+\ddot{z}) = \frac{2c_pI}{b(2l_b+l_m-l_e)}S. \tag{3.20}$$

Simply replacing equation (3.20) into (3.18) gives

$$z = S\frac{l_b^2}{3b}\frac{(2l_b+\frac{3}{2}l_m)}{(2l_b+l_m-l_e)}. \tag{3.21}$$

We can consider k_2 as connection for z and S that was presented in equation (3.21). A constant k_2 is therefore written as

$$k_2 = \frac{l_b^2}{3b}\frac{(2l_b+\frac{3}{2}l_m)}{(2l_b+l_m-l_e)} \tag{3.22}$$

and $z = k_2S$. The displacement component in equation (3.14) may be substituted with strain using this relation. The final interpretation is

$$\sigma_m = k_1 k_2 m \ddot{S} \tag{3.23}$$

Returning to equation (3.5), L_m may now be represented as follows: (3.24).

$$L_m = k_1 k_2 m. \tag{3.24}$$

In Figure 3.2, the resistive element indicates damping or mechanical waste. As stated in equation, the standard mechanical damping coefficient, bm, links force to velocity (3.25).

$$F_{bm} = b_m \dot{z}. \tag{3.25}$$

The analogous resistance, R_b, is a connection for stress σ and the rate of strain $\ddot{S}$. Force and velocity may be simply substituted with stress and strain rate by using the constants k_1 and k_2, as illustrated below.

$$\frac{\sigma_{bm}}{k_1} = b_m k_2 \dot{S}. \tag{3.26}$$

The formulation of R_b can be written as

$$R_b = k_1 k_2 b_m \tag{3.27}$$

where b_m is typical unit, that is: N s m^1.

Compliance is demonstrated by an element of capacitance in Figure 3.2. The compliance constant, s, or the inverse of the elasticity, c_p, is thus just the analogous capacitance, C_k, linking stress to strain.

Therefore, at zero strain, the transformer links stress (T) to voltage (V) [35]. When this assumption (zero strain) is applied to the piezoelectric constitutive connection in equation (3.3), the following equation is obtained:

$$T = -d_{31} c_p E. \tag{3.28}$$

Through the bender with two-layer , electric field and voltage can be connected in that way which is demonstrated in equation below

$$E = \frac{\alpha V}{2t_c}. \tag{3.29}$$

where a = 1 if the device's two layers are connected in series and a = 2 if they are connected in parallel. Simply replacing equation (3.29) into equation (3.28) yields

$$T = \frac{-a d_{31} c_p}{2t_c} V. \tag{3.30}$$

Equation (3.30) clearly indicates that the transformer's analogous turns ratio, n, is

$$n = \frac{-ad_{31}c_p}{2t_c}. \tag{3.31}$$

As illustrated in Figure 3.2, the current, i, reflects the current created as a consequence of mechanical stress measured at zero electric field. When this condition (zero electric field) is applied to equation (3.4) and strain is substituted for stress, the result is

$$D = d_{31}c_pS. \tag{3.32}$$

Keeping in mind that electrical displacement is nothing more than charge density across a dielectric material, electrical displacement may be linked to current for the bending device shown in Figure 3.1 by

$$i = a\omega l_e\dot{D} \tag{3.33}$$

Simply replacing equation (3.33) into equation (3.32) results in

$$i = a\omega l_e d_{31}c_p\dot{S} \tag{3.34}$$

This should also be emphasized that the bender's capacitance is provided by

$$C_b = \frac{a^2\varepsilon\omega l_e}{2t_c}. \tag{3.35}$$

By inserting the formulations for σ_{in} (equation (3.13), L_m (3.24), R_b (3.27), $C_k = c_p^{-1}$, n (3.31), i (3.34), and C_b (3.35) into formulas (3.5) and (3.6) and rearranging components, a workable modeling approach may now be produced. A system of equations that are corresponding to the stationary variables S, $\dot{S}$, and V are shown below.

$$\ddot{S} = \frac{-c_p}{k_1k_2m}S - \frac{b_m}{m}\dot{S} + \frac{c_p}{k_1k_2m}\frac{d_{31}a}{2t_c}V + \frac{\ddot{y}}{k_2} \tag{3.36}$$

$$\dot{V} = \frac{2t_cd_{31}c_p}{a\varepsilon}\dot{S} \tag{3.37}$$

The expression c_p/k_1k_2 refers to the relationship between force and vertical displacement and is often referred to as the equivalent spring constant, k. Equations (3.36) and (3.37) may be stated in state space form by substituting k for c_p/k_1k_2 as illustrated below:

$$\begin{bmatrix}\dot{S}\\ \ddot{S}\\ \dot{V}\end{bmatrix} = \begin{bmatrix}0 & 1 & 0\\ \frac{-k}{m} & \frac{-b_m}{m} & \frac{kd_{31}a}{2mt_c}\\ 0 & \frac{2t_cd_{31}c_p}{a\varepsilon} & 0\end{bmatrix} + \begin{bmatrix}0\\ \frac{1}{k_2}\\ 0\end{bmatrix}\ddot{y} \tag{3.38}$$

Three key suggestions have been made in the construction of this model. Starting with the mass on the beam's end which is supposed to operate like a point load which positioned at mass center (can be midway across the mass). A consequence of such assumption, no

allowance has been made for the condition that the slopes of the beam under the mass are same at all points. Second, the moment imparted on the beam by the proof mass's rotating inertia was ignored. This impact is greatest for the basic vibration mode, which is the sole vibration mode considered. Therefore, these two assumptions may result in minor mistakes. Eventually, the beam's mass was ignored. This is a sensible assumption that was discussed, because taken values are the bender sizes and proof masses.

The resistive load model

A model constructed above in section 3 does not include any electrical load. As a result, there is no power transmission. To evaluate how much power can be given to an actual electrical load, a basic resistive load may be used. Figure 5 depicts the resultant equivalent circuit diagram.

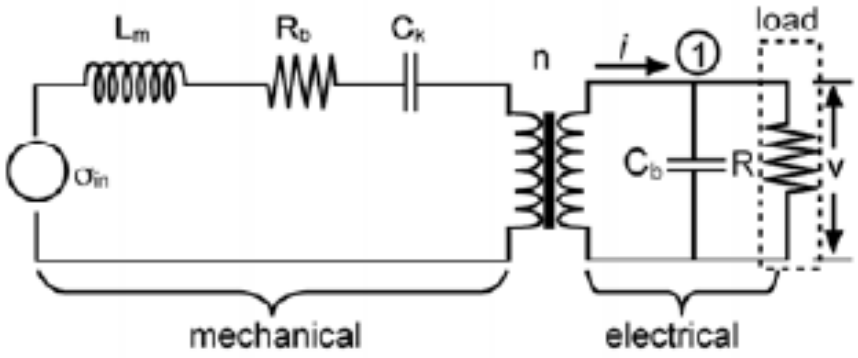

Figure 3.5: A piezoelectric generator with a resistive load is represented by a circuit diagram. [34]

Because the mechanical side of the corresponding circuit remains intact, equations (3.5) and (3.36) remain unaltered. In instead of equation (3.6), adding the currents now produces equation below at node 1:

$$i = C_b\dot{V} + V/R \tag{3.39}$$

The current i to be specified as continues equation, and simply replacing equation (3.34) for equation (3.39) and rearranging components results in the following equation instead of equation (3.37):

$$\dot{V} = \frac{2t_c d_{31} c_p}{a\varepsilon}\dot{S} - \frac{1}{RC_b}V. \tag{3.40}$$

The derived state space system equations are therefore

$$\begin{bmatrix} \dot{S} \\ \ddot{S} \\ \dot{V} \end{bmatrix} = \begin{bmatrix} 0 & 1 & 0 \\ \frac{-k}{m} & \frac{-b_m}{m} & \frac{kd_{31}a}{2mt_c} \\ 0 & \frac{2t_c d_{31} c_p}{a\varepsilon} & \frac{-1}{RC_b} \end{bmatrix} + \begin{bmatrix} 0 \\ \frac{1}{k_2} \\ 0 \end{bmatrix} \ddot{y} \tag{3.41}$$

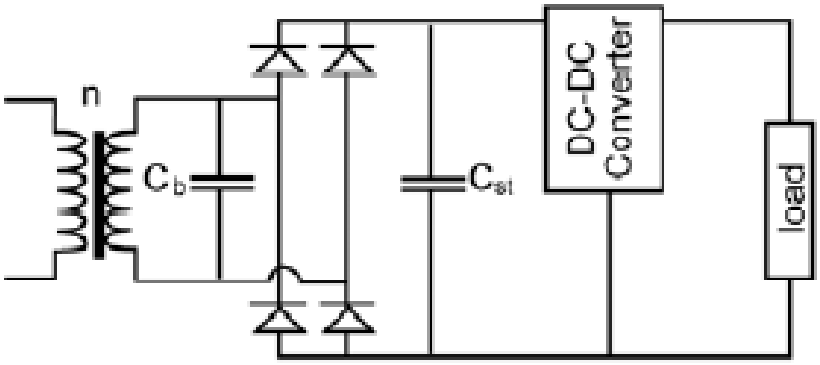

Figure 3.6: A piezoelectric generator that includes power circuits and a load. There is no corresponding circuit for mechanical items presented. [34]

The model in equation (3.41) may be used to produce an analytical statement for power transmitted to a resistive load . An analytical statement of this kind is important not just for calculating power, but also for providing the developer with additional insight about the system. The resistive load dissipates power as V^2/R. As a result, from equation, an analytical expression for V must be derived (3.41). Applying the Laplace transform of equation (3.40) and adjusting the components produces

$$S = \frac{a\varepsilon}{c_p d_{31} t_c s}\left(s - \frac{1}{RC_b}\right)V \tag{3.42}$$

where s is the Laplace factor and S and V represent strain and voltage in the time and frequency domains, respectively. Assuming the Laplace transform of equation (3.36), adding the corresponding spring constant k, and rearranging the components results in

$$S\left(s^2 + \frac{b_m}{m} + \frac{k}{m}\right) = \frac{akd_{31}}{2mt_c}V + \frac{A_{in}}{k_2} \tag{3.43}$$

where A_{in} iis the acceleration-based Laplace transform of the input vibrations. Substituting equation (3.42) into equation (3.43) and rearranging terms yields the following expression:

$$V\left[s^3 + \left(\frac{1}{RC_b} + \frac{b_m}{m}\right)s^2 + \left(\frac{k}{m}\left(1 + \frac{d_{31}^2 c_p}{\varepsilon}\right) + \frac{b_m}{mRC_b}\right)s + \frac{k}{mRC_b}\right] = \frac{2c_p d_{31} t_c}{k_2 a\varepsilon}sA_{in} \tag{3.44}$$

For the magnitude of the output voltage, the statement in equation (3.44) may be solved. The replacements undertaken below may make highly significant the resultant phrase : $d_{31}^2 c_p/\varepsilon$ is term's square, where the coefficient of piezoelectric coupling is indicated in terms of k_{31}, in which the Laplace variable is written in terms of $j\omega$, and j is represented as an imaginary number, and for a squared system k/m can be denoted as a natural frequency, where the system itself is demonstrated in terms of ω_n^2, also there is a term b_m/m which is damping and it is represented in terms of the unitless damping ratio η as

$2\eta\omega_n$. Performing these modifications and calculating for V results in

$$V = \left\{ j\omega \frac{2c_p d_{31} t_c}{a\varepsilon} \frac{A_{in}}{k_2} \right\} \left\{ \left[\frac{\omega_n^2}{RC_p} - \left(\frac{1}{RC_b} + 2\zeta\omega_n \right) \omega^2 \right] + j\omega \left[\omega_n^2 \left(1 + k_{31}^2 \right) + \frac{2\zeta\omega_n}{RC_b} - \omega^2 \right] \right\}^{-1}. \tag{3.45}$$

If we make the additional calculations easier that the resonance frequency, ω_n, equals the driving frequency, ω, that gives us a simplified equation (3.45)

$$V = \frac{j\omega \frac{2c_p d_{31} t_c}{a\varepsilon}}{j\omega \left(\omega^2 k_{31}^2 + \frac{2\zeta\omega}{RC_b} \right) - 2\zeta\omega^3} \frac{A_{in}}{k_2} \tag{3.46}$$

Simply stated, there is rms (root mean square) power given as $|V|^2/2R$ and it is transmitted into resistive load. As a consequence of utilizing the formula in equation (3.46), this expression of rms power will be given in terms of following equation

$$P = \frac{1}{2\omega^2} \frac{RC_b^2 \left(\frac{2c_p d_{31} t_c}{k_2 a\varepsilon} \right)^2 A_{in}^2}{\left(4\zeta^2 + k_{31}^4 \right) \left(RC_b\omega \right)^2 + 4\zeta k_{31}^2 \left(RC_b\omega + 4\zeta^2 \right)}. \tag{3.47}$$

The optimal load resistance may therefore be calculated by solving for R and differentiating equation (3.47) which leads to Equation (3.48) that depicts the most optimal load resistance as a consequence .

$$R_{opt} = \frac{1}{\omega C_b} \frac{2\zeta}{\sqrt{4\zeta^2 + k_{31}^4}}. \tag{3.48}$$

The capacitive load model

The preceding study is beneficial since it is founded on a basic resistive load, but it is not a particularly exact approximation of the true electrical load. If we consider it in practice, the electrical system might match the circuit as demonstrated in Figure 3.6. Consider that Figure 3.6 does not depict the mechanical side of the circuit, despite the fact that it is the same as in Figures 3.2 and 3.5. In deal,instead of the storage capacitors C_{st} it can be replaced by battery which is rechargeable.

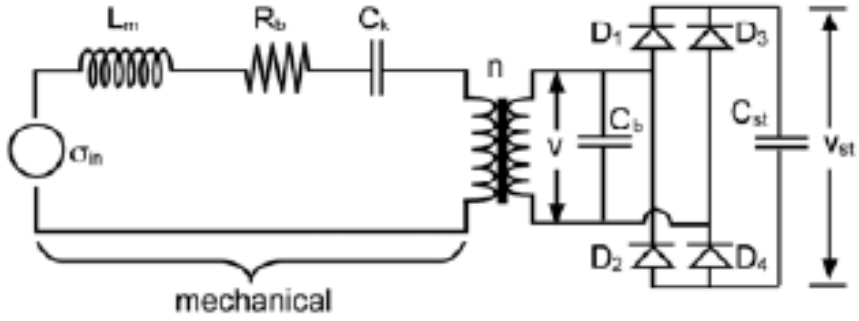

Figure 3.7: A simple circuit diagram used to examine the charging of the storage capacitor. [34]

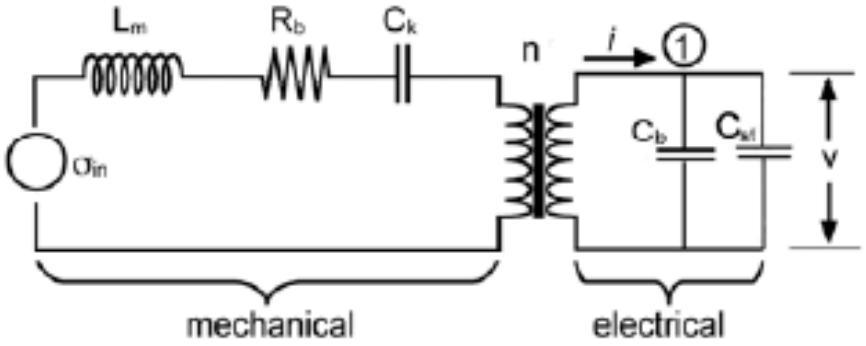

Figure 3.8: State 1 equivalent circuit diagram with diodes D1 and D4 conducting. [34]

The radio IC in wireless sensor systems will normally switch on for a brief amount of time, receive and send data, and then turn off or be in sleep state. Usual duty cycles are estimated to be approximately 1 % [37].

As a result, the radio IC is inactive state 99 % of its work and just uses a small amount of current; and the DC–DC converter is turned off while it is inactive state. As a result, the vibration converter only charges the storage capacitor 99 % of the time. Figure 3.7 depicts a simplified circuit representation for this scenario. The creation of a model for this situation is beneficial since it depicts a more accurate operating state.

The circuit seen in Figure 3.7 may function in three different states. Condition 1 will refer to the current state of diodes D1 and D4. Condition 2 will relate to the current state of diodes D2 and D3. Eventually mode 3 can indicate the absence of these four diodes that are rectificated . To simplify the study, an ideal diode model is utilized.

The initial system equation, presented in the sections before like in equation (3.36), is unaltered in any of the three phases. The corresponding circuit at phase 3 (there is no diodes conducting) is same as illustrated for Figure 3.2, hence system for two equations in second state is same that was demonstrated in equation (3.37). Eventually for phase 3, the voltage value V_{st} remains constant. Figure 8 depicts the comparable circuit representation for phase 1. Equation (3.49) 1 is the second of two system equations for phase 1. In phase

1, the storage voltage V_{st} equals the voltage all over the piezoelectric element, V. In the equation (3.49) second system equation for phase 2 is the same as the first system equation for phase 1. However, in phase 2, V_{st} = - V. Hence, for phases 1 and 2, the system model is provided by equations (3.36) and (3.49) and for phase 3, by equations (3.36) and (3.37).

$$\dot{V} = \frac{ac_p d_{31} l_e \omega}{C_b + C_{st}} \dot{S}. \tag{3.49}$$

Model for different beam configurations

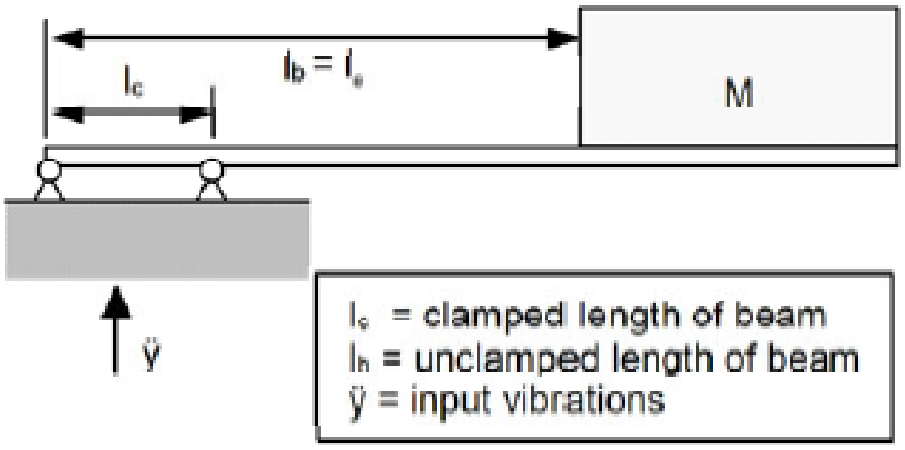

Figure 3.9: Pin–pin mounting is used to represent a clamped beam. [34]

When examining various beam mounting arrangements, the benefit of deriving the constants k_1 and k_2 above is easily apparent. That is there is a unique formulas linking average stress expression with input force (k_1) given, also the average strain formulation with vertical displacement (k_2) vary from the basic model. As a result, the models shown in equations (3.38), (3.41), and (3.49) are typically true for a bender installed in the majority of beam configurations. Therefore, the equations for k_1 and k_2 will alter depending on the mounting circumstance. Below is a quick discussion of an exemplary case.

The analysis implies that the beam's mounting structure is fully stiff. In practice, the mounting structure will be somewhat compliant. The benders have been clamped in practice. The pin–pin mounting, as illustrated in Figure 3.9, was shown to be a more realistic model for the beam, particularly for extremely tiny (short) designs. The denoted beam length l_c on which the clamp is in the top of given length. The length given for the electrode, l_e, can also be considered as same with the beam's whole length which is in deal in accordance with the proof mass, l_b. Expressions for k_1 and k_2 are obtained in the same way as explained previously. Equations (3.50) and (3.51) illustrate the resultant formulas for the pin–pin model (3.51). The preceding models for no load, resistive load, and capacitive load may now be applied by easily entering the new formulas for the constants k_1 and k_2:

$$k_1 = \frac{b(4l_b + 3l_m)}{4I} \tag{3.50}$$

$$k_2 = \frac{l_b(l_c + l_b)}{3b} \tag{3.51}$$

3.2 Design of Piezoelectric Energy harvesting device

According to equation (3.45), (3.46), (3.47) from state-space model of a system an analytical expression for power have been transmitted to a resistive load. Equation (3.46), (3.47) are the analytical expressions of output power and voltage, that is why further design of a cantilever beam has been made in accordance to analytical solutions.

First of the all it is significant to know that a Piezoelectric Harvester Devices operate only around resonance frequency which is $\omega_n = \sqrt{k/m}$ (natural frequency). Which is important take into account according to S. Roundy [34] that in analytical solution of the system resonant frequency is equals to frequency input ($\omega_n = \omega$). This is first step to start design.

In the Figure 3.10 excitation data of a operating pipeline pump. According to this figure mean value of frequency has been taken and implemented to analytical solution of the system.

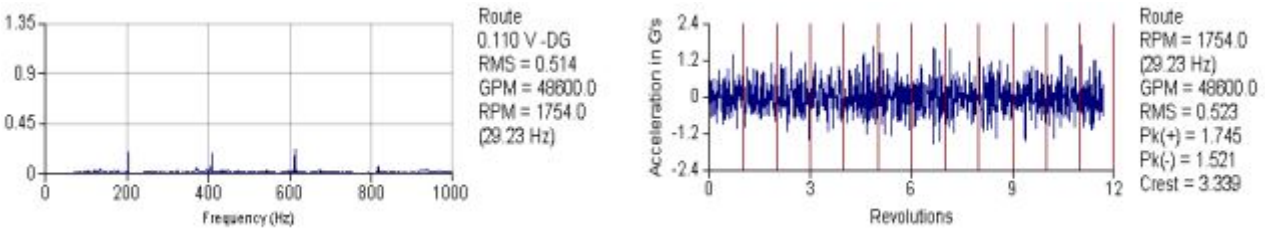

Figure 3.10: Vibration data of an operating pump at 48600 GPM Flow

From this equality of resonant frequency and input frequency, we get many variables of the geometry of a cantilever beam and mass. According to the analytical solution of output power the only non-material parameters are t_c, k_2 and $\omega \cong \omega_n$. As it is obvious that too many geometrical variables appear, first thing to do is to build a cantilever beam with bimorph piezoelectric structure which should provide with an optimal output power in accordance to S. Roundy [34] which is approximately $180 - 200$ $[\mu W]$.

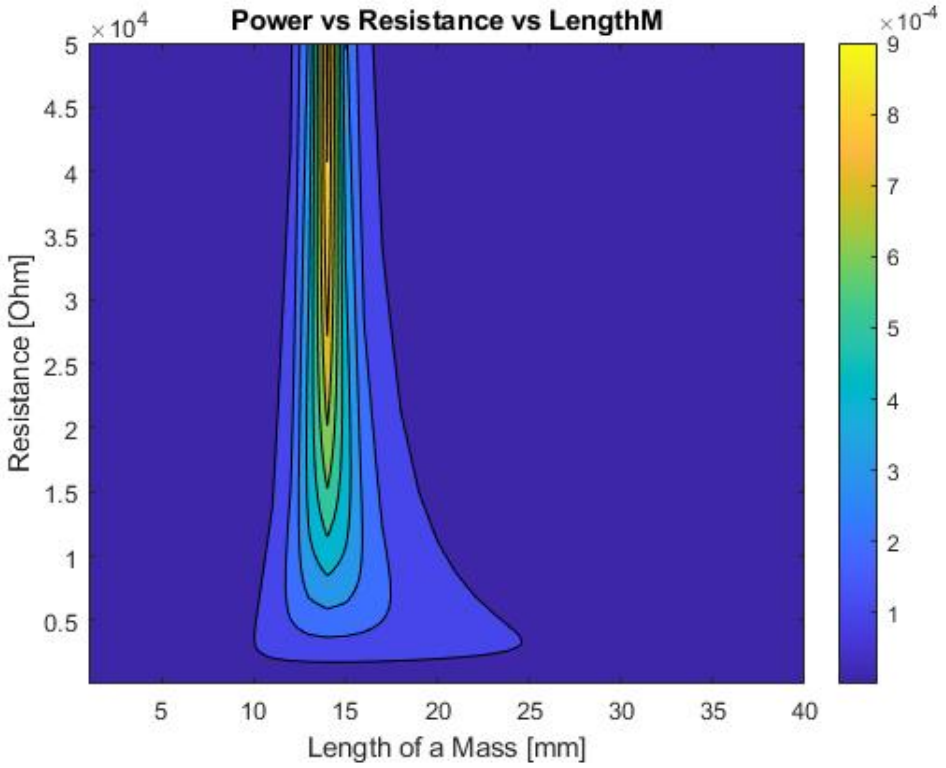

Figure 3.11: Power × Resistance × Mass Length $[mm]$

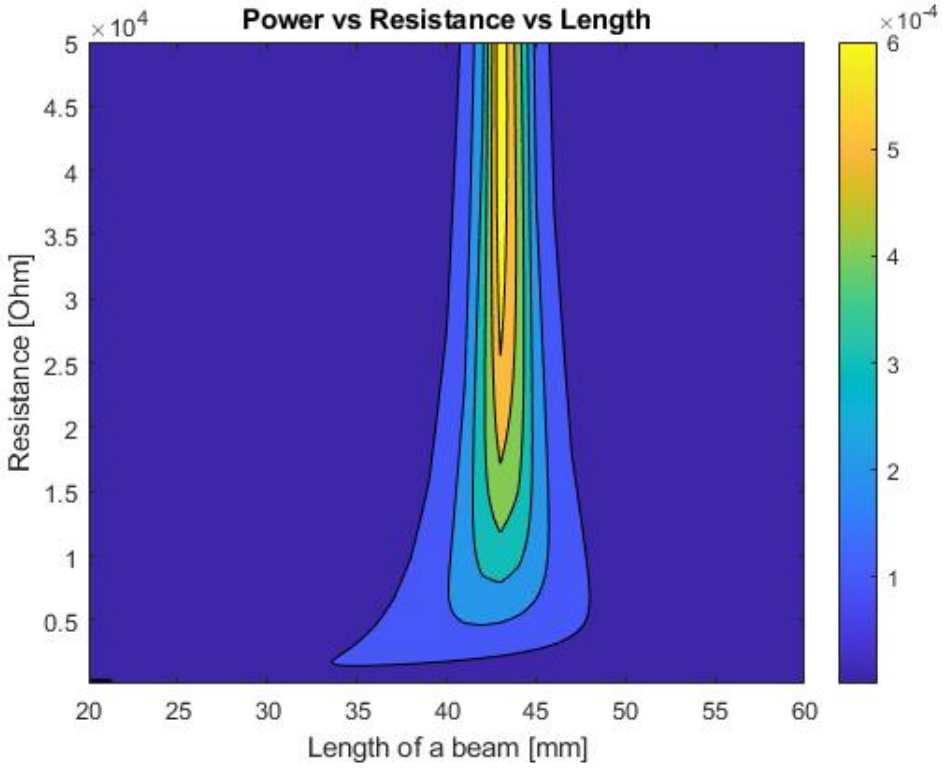

Figure 3.12: Power × Resistance × Length of a cantilever beam $[mm]$

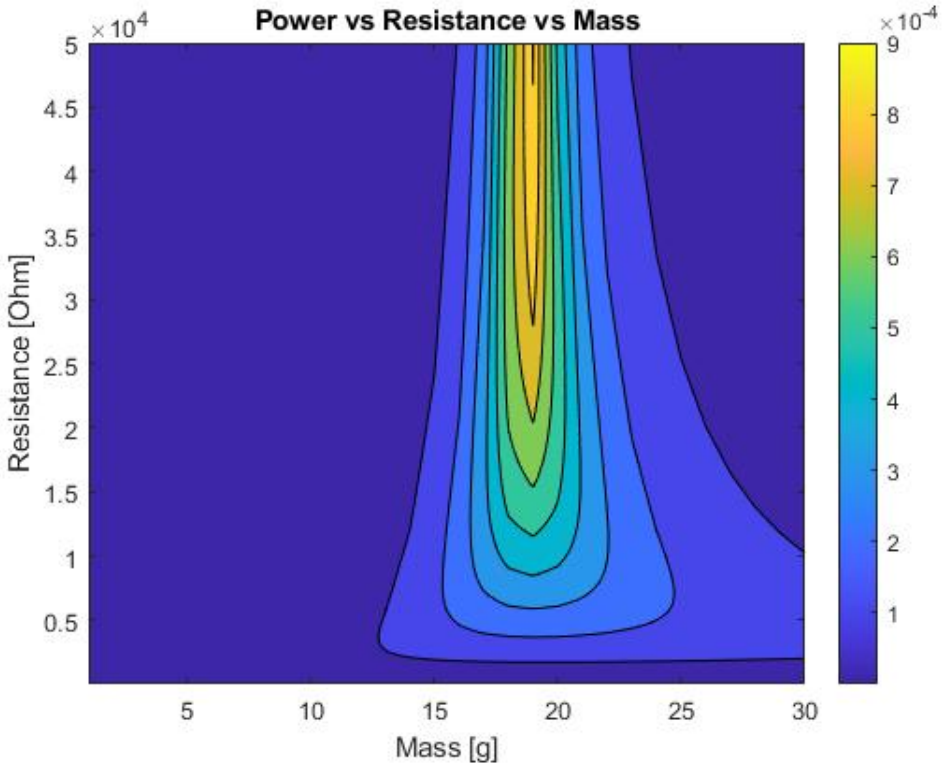

Figure 3.13: Power × Resistance × Mass $[g]$

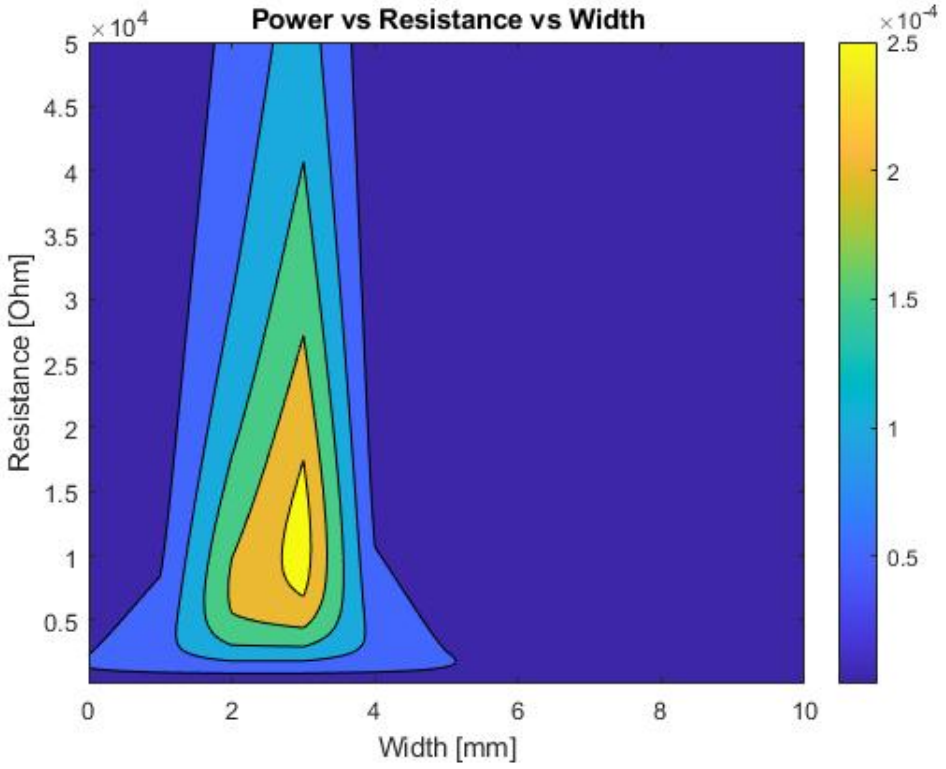

Figure 3.14: Power × Resistance × Width of a cantilever beam $[mm]$

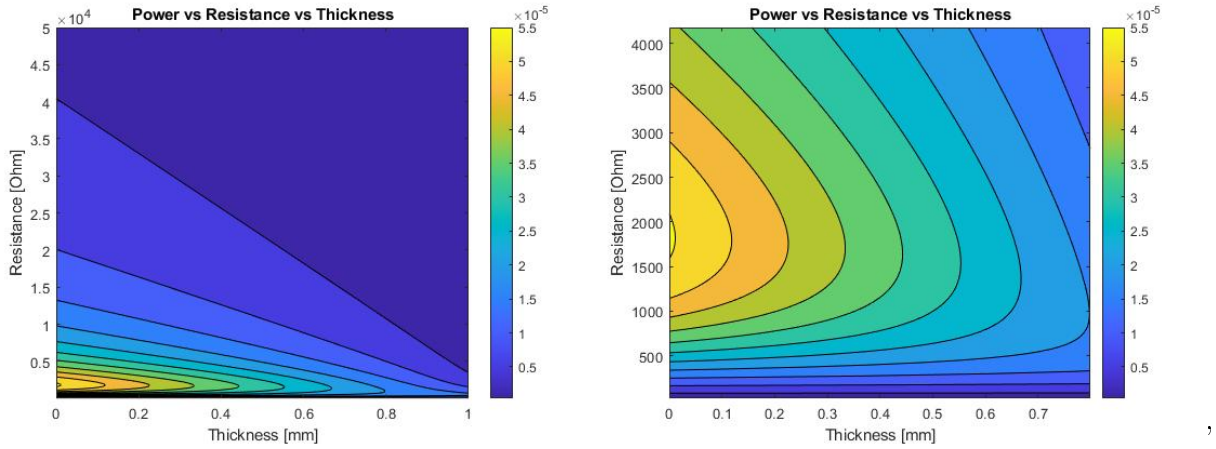

Figure 3.15: Power × Resistance × Thickness of a cantilever beam [mm]

Figures 3.11, 3.12, 3.13, 3.14, 3.15 are the contour diagram with 3 variables every time taking some other variables as a constant value, another changing geometry properties has been found by this way in order to create design that will provide with optimal output power.

The first simulation made according to S. Roundy's [34] the output power and voltage are shown in the Figure 3.16.

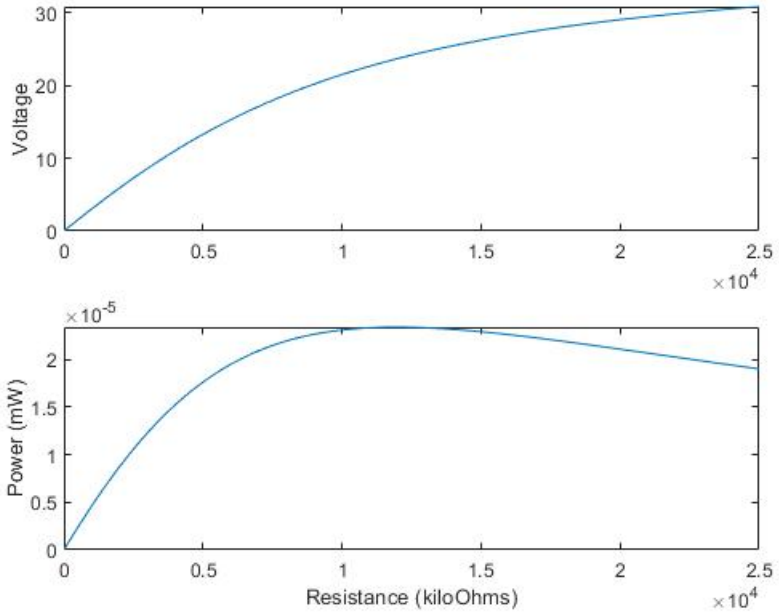

Figure 3.16: First simulation of the analytical model

Many mistakes and errors were made in the material parameters and this is why the output power was so low. This is not the optimal value that should be got and model should be developed and optimized.

Finally, optimized numerical simulation of the model has been completed. Figure 3.17 is a diagram of the output *Voltage* and *Power* with the optimal design of a piezoelectric cantilever beam with a fixed one-clamped length.

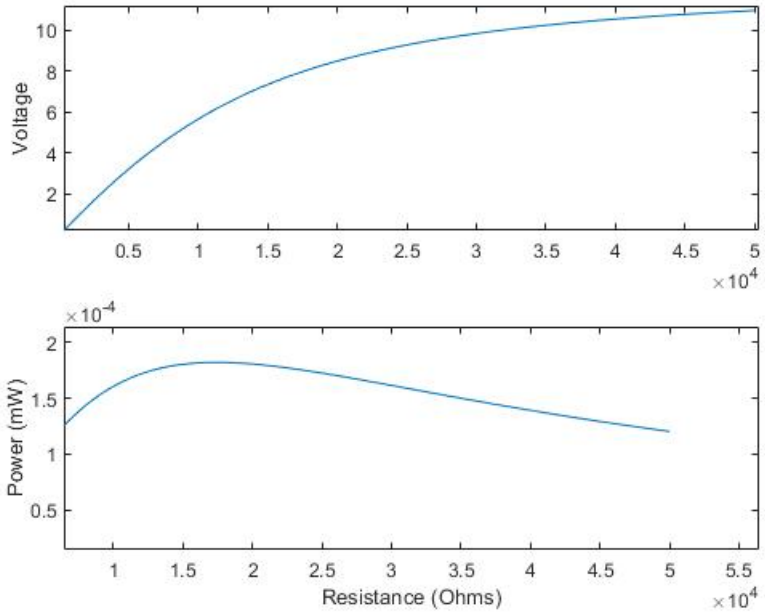

Figure 3.17: Output Voltage and Power plot of an optimal model of a Numerical simulation

The further design and optimization were made according to this numerical simulation of an analytical model and compared to the model that was presented by S. Roundy [34].

In the Table 3.1 parameters of a optimal Piezoelectric Energy Harvesting (Cantilever beam type) are shown. As an input parameter it has been taken into account excitation at 2.5 $m\ s^{-2}$ at 120 hz. These parameters are taken from the provided data by Flowserve INC in the Figure 3.18.

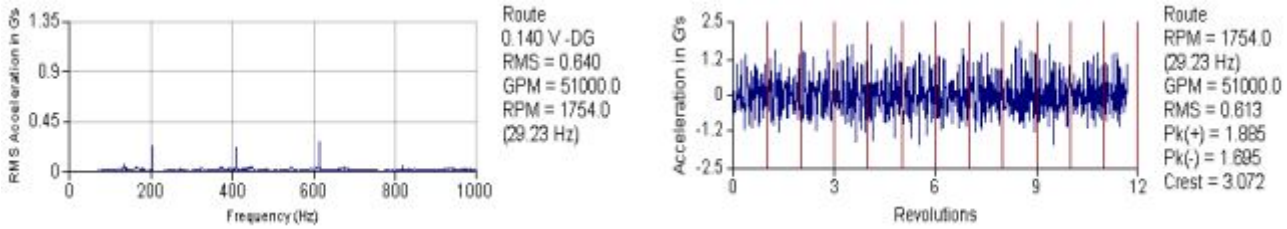

Figure 3.18: Vibration spectrum of an operating pipe-line pump at 51000 GPM flow

Substrate material (Shim)	Steel
Young's modulus (GPa)	190
Poisson's ratio μ_s	0.23
Density kg^3	7750
$Length \times width \times thickness(mm)$	18 $\times$3.1 $\times$ 0.102
Piezoelectric material	PZT-5A
Young's modulus:	
E_{11}	66
E_{33}	54
Poisson's ratio	0.34
Density ρ (kg/m_3)	7800
Piezoelectric constants $(\times 10_{12} m/volt)$:	
d_{11}	390
d_{31}	-190
Coupling coefficients:	
k_{33}	0.72
d_{31}	0.35
Relative dielectric constant ϵ_{33}	1800
Mechanical quality factor Q_m	80
$Length \times width \times thickness(mm)$	30.35 $\times$3.2 $\times$ 0.15
Mass	Tungsten
Young's modulus (GPa)	190
Poisson's ratio	0.28
Density ρ (kg/m_3)	19300
$Length \times width \times thickness(mm)$	8.5 $\times$7.7 $\times$ 6.7

Table 3.1: Design and Material parameters that have been simulated for optimization according to [34]

Material parameters of a piezoelectric (PZT-5A) are taken from https://support.piezo.com . According to progressed data and geometry of a PEH, the design of a cantilever beam has been set and shown in the Figure 3.19. After proper design I tried to make a computational modal analysis of a cantilever beam to see mode-shapes and optimal input vibration which can provide more output Power.

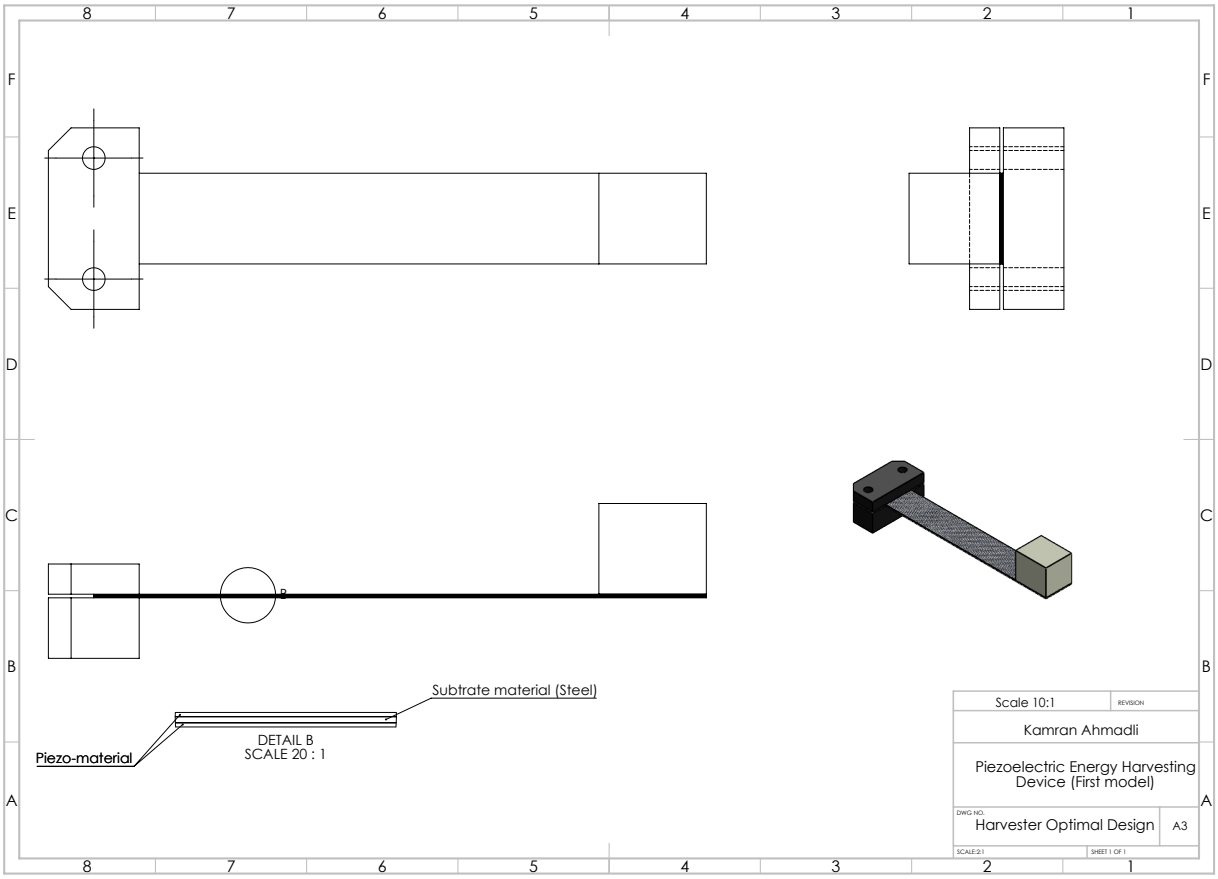

Figure 3.19: First optimal design of a PEH (cantilever type)

After the final design which was succesfully done according to analytical model derived by Roundy and Wright [34], I have decided to try increase output power, by changing input settings. To do so I have changed beam parameters such that I put shorter beam that will increase resonant frequency ω_n to value of 204.6158 Hz. After which i set values of driven frequency around natural frequency to see the output power spectrum, because it is important that $\omega_n \simeq \omega$. In the Figure 3.20 it is shown that optimal power in the different frequency range can be obtained.

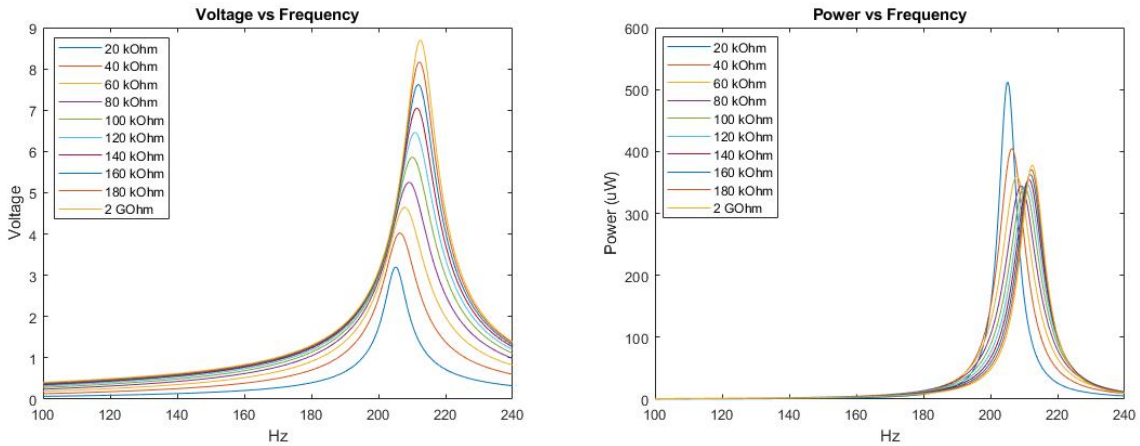

(a) (b)

Figure 3.20: Frequency range of operation of a Piezoelectric Energy Harvesting device

Figure 3.21 shows Modal analysis of a cantilever beam that have been modeled in ANSYS. The solid model was created and tetrahedral mesh was applied for the structure. As a boundary conditions clamped part of a beam was fixed at the end of the model by applying zero displacement for all DoF at the nodes. Beam itself was done as 3 layers and as a material it was chosen PZT and Brass for middle layer from material library of ANSYS. Solver was chosen as a Modal Analysis to determine natural frequencies of first mode shapes of a model.

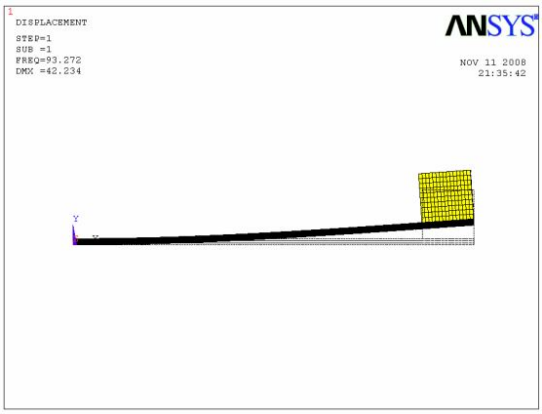

(a) First mode-shape

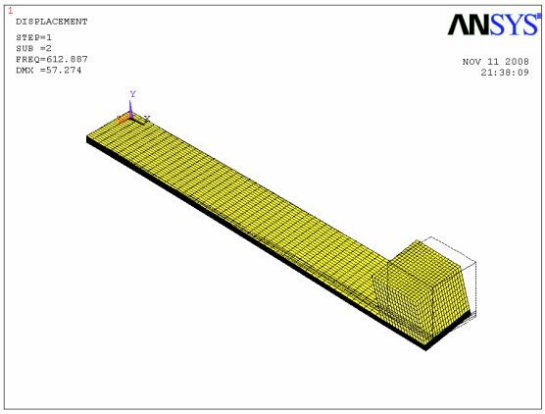

(b) Second mode-shape

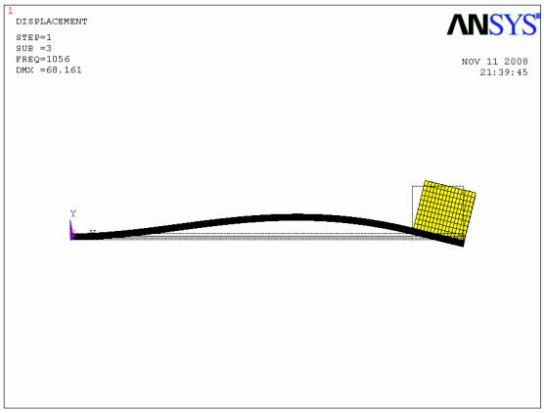

(c) Third mode-shape

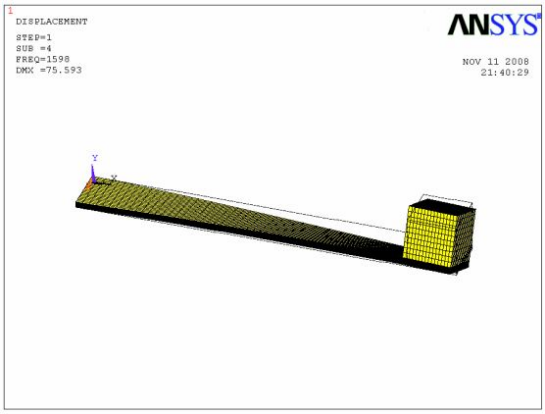

(d) Fourth mode-shape

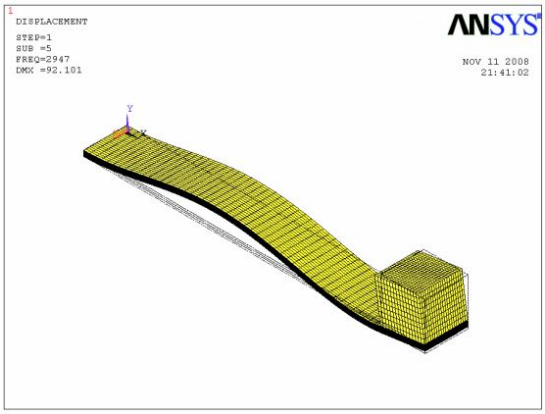

(e) Fifth mode-shape

Figure 3.21: Computational Modal Analysis of a cantilever beam with proof mass at the end (first 5 mode-shapes)

3.3 Analysis of different designs of Devices

Developed design of a Bimorph Piezoelectric Energy Harvesting Device

In this section my own design of a Piezoelectric Energy Harvester will be presented. The most optimal parameters of a cantilever beam explored and implemented, the proper materials have been chosen. The aim of this is to get higher output power with a higher input frequency of 400 Hz, taken from the data of the operating pipeline pump (Mean value of the frequency has been taken) Figure 3.22.

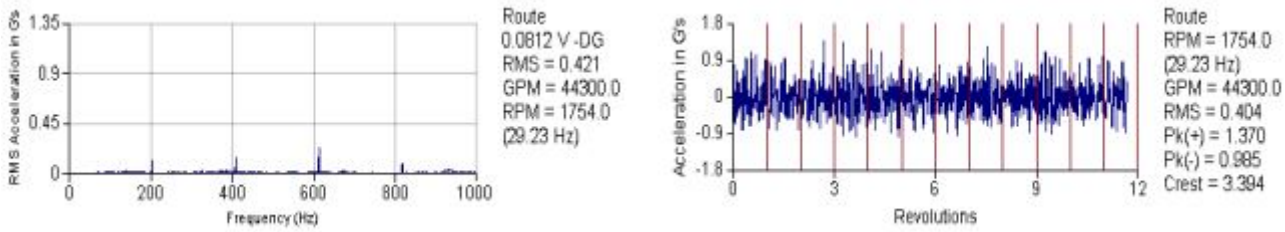

Figure 3.22: Vibration spectrum of an operating pipe-line pump at 44300 GPM flow

This time design were provided to get higher power output. Table 3.2 shows all the parameters found for the best results. Steps were taken as in the previous section. This time as an input frequency was 400 Hz.

Figure 3.23 indicates $Power, Voltage - Resistance$ diagram of a this design of PEH. In the Figure 3.24 shown all the details of the PEH, cantilever beam parameters (drawing).

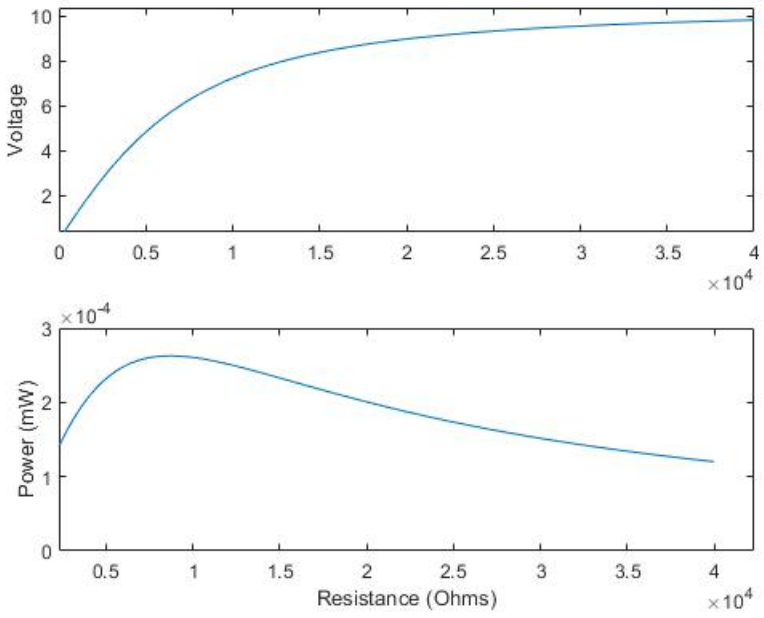

Figure 3.23: Output Voltage & Power plot of a developed model of a Numerical simulation

Substrate material (Shim)	brass
Young's modulus (GPa)	110
Poisson's ratio μ_s	0.23
Density kg^3	2330
$Length \times width \times thickness(mm)$	40.6 $\times$3.1 $\times$ 0.102
Piezoelectric material	PSI-5H4E
Young's modulus:	
E_{11}	62
E_{33}	50
Poisson's ratio	0.3
Elastic constants (GPa):	
C_{11}	110.8
C_{12}	49.8
C_{13}	49.8
C_{33}	110.8
C_{44}	30.5
Density ρ (kg/m_3)	7800
Piezoelectric constants ($\times 10_{12} m/volt$):	
d_{11}	650
d_{31}	-320
Coupling coefficients:	
k_{33}	0.75
d_{31}	0.44
Relative dielectric constant ϵ_{33}	3800
Mechanical quality factor Q_m	32
$Length \times width \times thickness(mm)$	40.6 $\times$3.1 $\times$ 0.278
Mass	Tungsten
Young's modulus (GPa)	400
Poisson's ratio	0.28
Density ρ (kg/m_3)	17000
$Length \times width \times thickness(mm)$	12 $\times$8.2 $\times$ 9.4

Table 3.2: Design and Material parameters

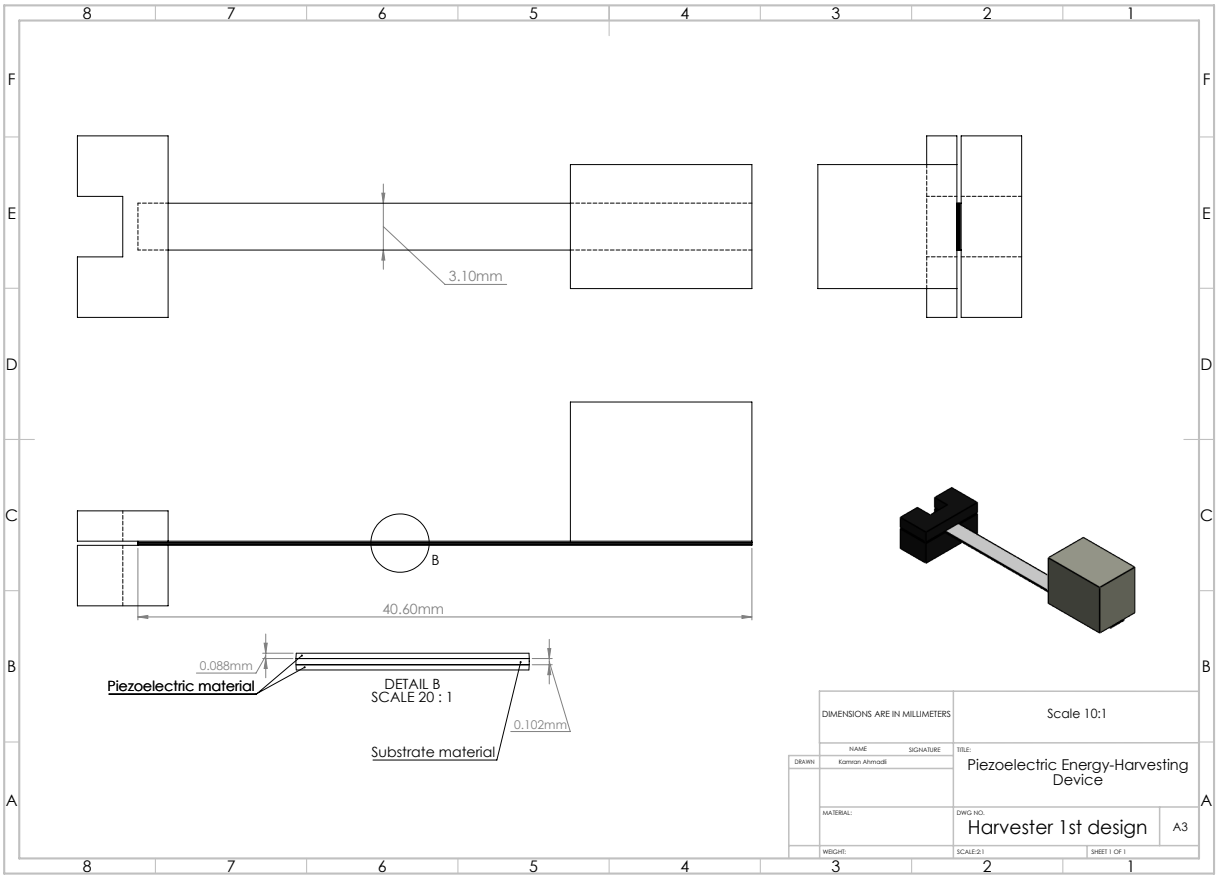

Figure 3.24: Developed design of a Piezoelectric Energy Harvesting device

This time, it was also decided to determine the highest power output that can be achieved with various frequencies. However, as a case, it has been selected optimal frequency input of 400 Hz at an input amplitude of 2.5 $m\ s^{-2}$. This was explored for the purpose of research for future generation high-power sensors, although the energy harvesters should be designed for low-powered circuits. Figure 3.25 shows us a graph of $Power - Resistance$ to understand that Piezoelectric Energy Harvesters can reach high power output with optimal Resistance $2.3892 * 10^5$ $Ohms$.

As the next design it will be discussed and analyzed about high power generation Piezelectric Device that was designed and suggested by M. Zhu et al. [32]. This is a promising development that will allow EHDs to be used in a larger variety of applications. Furthermore, physical insights into how each parameter affects output power are examined in depth.

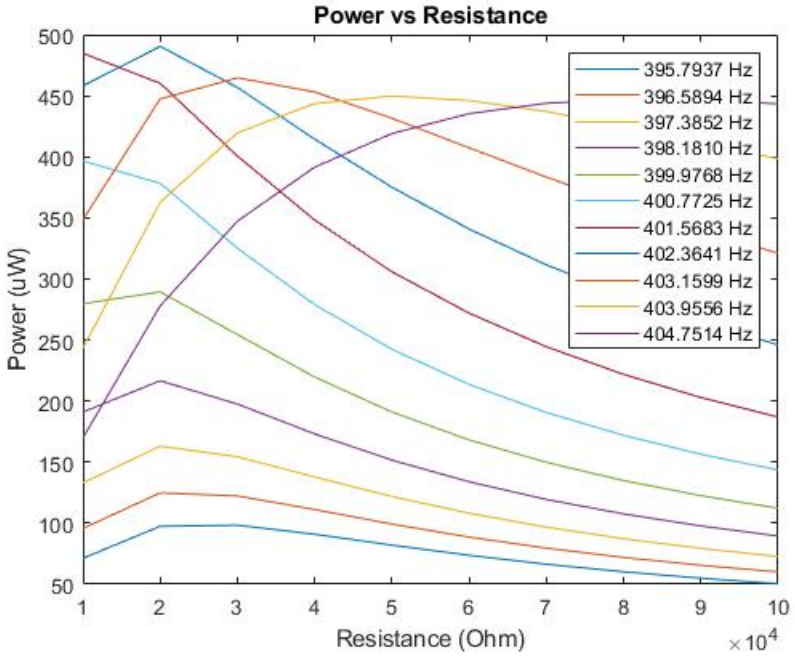

Figure 3.25: Power - Resistance graph at different frequency values of the first design.

Suggested Design for Higher Electrical Power Circuits

This design was suggested, explored and provided experimental analysis by M. Zhu [32]. Aim of this research was to provide an optimal FEM analysis of a cantilever beam, ensure proper design and obtain values of the current flowing through the load resistor and the voltage formed across it, the power dissipated by the resistor and the resulting vibrational displacement amplitude, and the resonant frequency, and value of optimal resistance. According to M. Zhu [32], in future sensors will be developed and operate with higher power and functionality.

The following strategies should be used when designing with the goal of generating more power in case of a cantilever beam: it is suggested to be shorter, wider and low thickness ratio of piezo-layer. For the tungsten-mass: it is better to design mass with shorter mass length and higher in height. In final analysis of such design up to 2.5 mW/cm^3 can be obtained which is significantly more than 200 $\mu W/cm^3$.

Figure 3.26 is suggested design with piezelectric beam length of 6 mm and at the end mass attached to substrate material with a length of $18mm$ with mass geometry at the end of a beam being $12mm \times 8.2mm \times 9.4mm$.

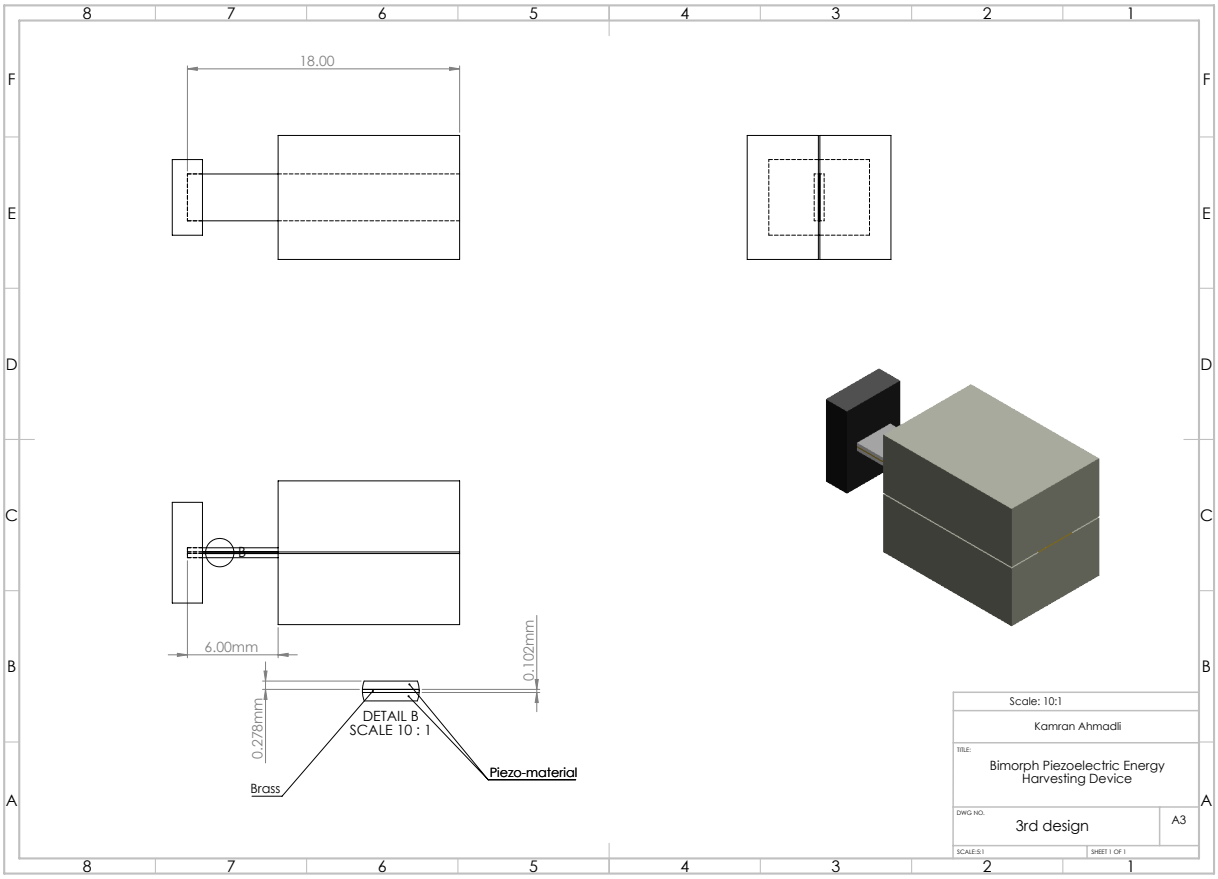

Figure 3.26: Piezoelectric Energy Harvester model suggested by [32]

Figures 3.27a and 3.27b are the plot diagrams of power/voltage output and current flow through the load resistance are expressed. As Figure 3.27a shows that analytically the power output can be reached up to 2.5 mW/cm^3 or exceed this value.

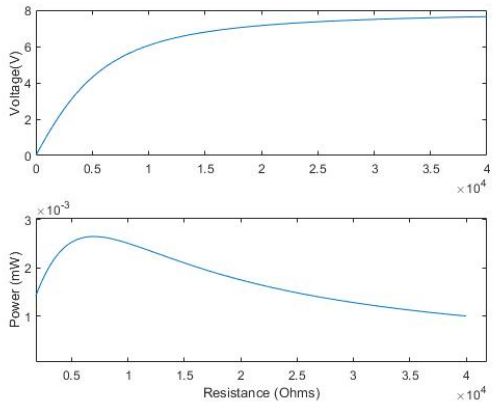

(a) Power & Voltage - Resistance plot

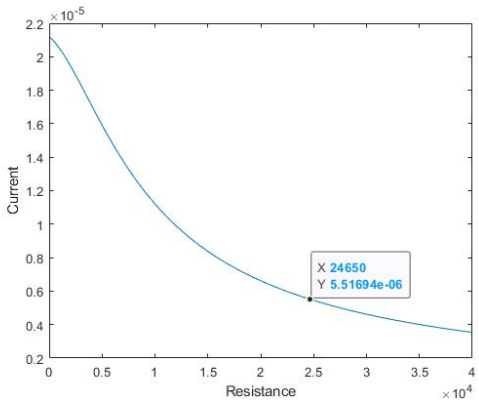

(b) Current - Resistance plot

Figure 3.27: Diagrams of an output Power, Voltage & Current of the model suggested by [32]

Chapter 4

Results and Discussion

In this chapter, the results of designed EHDs will be discussed and compared to the experimental outputs. Unfortunately, I was unable to conduct the experiments myself due to a variety of factors. As a consequence, the computational results will be compared to those of other authors who have succeeded in analyzing Piezoelectric Energy Harvesters experimentally.

4.1 Parametric Design Analyzes of a 2nd device (Developed design of a Bimorph Piezoelectric Energy Harvesting Device)

The purpose of this chapter, and specifically this section, is to examine the PEHD design in section 3.3. The author of this thesis has numerically analyzed, designed, and suggested the optimal design, Figure 3.24. Aim is to compare theoretical knowledge of Piezoelectric Energy Harvester to Computational results.

1) *Different length of a beam*: Figure 4.1 shows variation of Power (μW) and Voltage (V) with respect to the length of a cantilever beam. The measurements were taken to the optimal resistance of a value $2.6145 * 10^5$ $Ohms$. The motive of this plot to show how dissipated Power through resistance varies because of a change of the length of a beam. According to Figure 4.1 it is clear how l_b (length of a beam) affects to output Power and Voltage. As a beam length increases from 40.6 mm to 67 mm Power and Voltage decreases to 11 μW and 3 V respectively. And clearly in terms of [38], [32], and vibration theory [39], this outcome is comprehensible because Power is proportional to the resonant frequency (w_n). Natural frequency being in a relation with beam length ($w_n \sim \frac{1}{l_b^2}$), so as longer beam is as lower power output will be obtained.that is why when designing a piezoelectric EHD with the goal of generating a larger power output, a shorter beam is recommended.

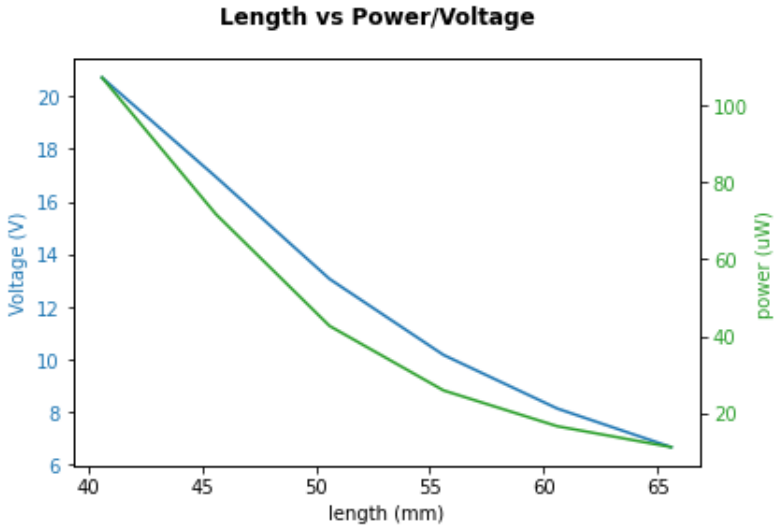

Figure 4.1

2) *Different width of a beam*: Figure 4.2a shows how Power (μW) increases and reaches 467.3 μW while we increase width of a beam, however in the Figure 4.2b it is indicated slight change of a Voltage (V) (almost does not change and remains around 9.7 V). This comes as an output Power is directly proportional to width w, and the wider the beam, the more power we can consume. And so width of a beam has a considerable effect on an output Power. This makes a design really easier as output Power can be increased without much change in resonance frequency.It makes matching the ambient vibration frequency considerably simpler while also allowing for an increase in the power output.

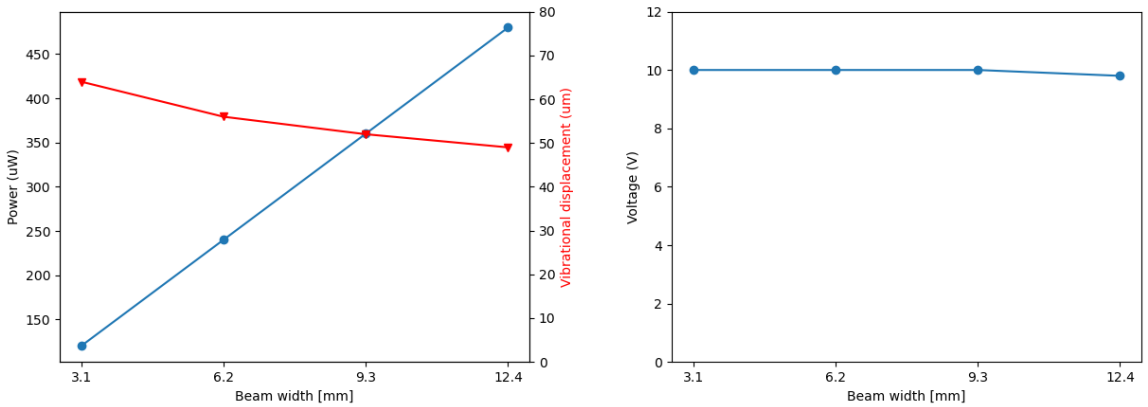

(a) (b)

Figure 4.2

3) *Different ratio of a piezoelectric layer thickness and total beam thickness* : Figure 4.3a shows how Voltage V increases as the ratio of a $\frac{t_p}{t}$ increases. However, in Figure 4.3b it seems that this ratio affects power only a little. It also should be mentioned that although Voltage increases current decreases in this case. This is why while designing

PEH, the thickness of a beam and coating of a beam with a thick or thin layer of piezo-material should be taken under consideration.

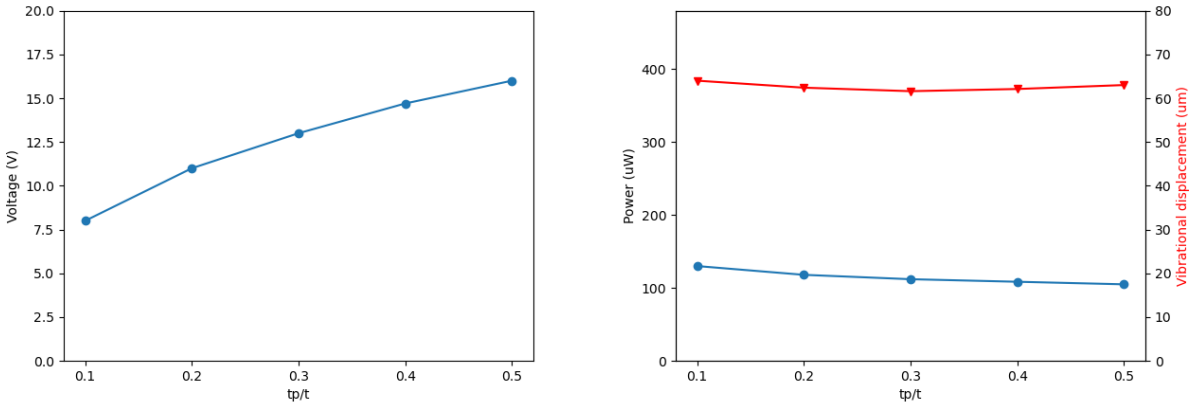

(a) (b)

Figure 4.3

4.2 Summary

The best way to summarize this chapter is to do a comparison of the optimal final design to the experimental methods and analytical approaches of different researchers. The experiments of S. Roundy and P. K. Wright [34] show the values of output power which can reach up to 200 μW comparing to this design in the Figure 3.17 that I have numerically simulated and also have got pretty close reults approximately Power reaching $180 \sim 190 \mu W$. I find this numerical computation and analyze successful. It is important to mention that in all three designs capacitance have been taken into consideration at a value of 9.2 nF. Second design's output power exceeds the 200 μW and reaches approximately 260 muW which is still reasonable value for the operation of low-powered sensors. Third design that was suggested by [32] is for next generation high powered sensors and was discussed only for the comparison and to show for future that PEHDs can reach Power values up to 2.5 mW.

To sum up, mathematical model has been derived and computationally simulated to show generally how it operates. After obtained idea the design have been developed for better use and more power output generated that can be useful for more cases. Both designs have been compared and discussed. For future model of the piezoelectric energy harvester it has been shown how geometry parameters affect output Power, Voltage and Current.

Chapter 5

Conclusion

The industry of oil production and its transportation is one of the greatest industries in the world. There is not much demand for pipeline pump consumption in this field of industry. The best method of transportation for crude oil and other chemicals is pipelines, which is the most efficient, cheapest, and safest method. Although all the benefits of pipelines and pipeline pumps are present, constant maintenance and control are required. This thesis outlines how pumps operate, some of the reasons for their damage, and the main energy losses of the pumps. The general and most convenient method to keep the process under control is remote controlled sensors. which sends all the collected data frequently to the MCU, so the operator can easily track all the systems under control. In this thesis, a revolutionary new system of wireless sensor networks has been researched, described, and discussed. The way wireless sensor networks operate, at which rate they work, and the fact is, nowadays, they are very helpful for pump condition monitoring.

This thesis was mostly focused on the Energy Harvesting Devices. As nowadays, control units' decrease on micro and macro scales, the consumption of power required also decreases. And this is why the development of Energy Harvesting Devices is needed and, in the future, they will probably be presented as devices to replace batteries and energy storage units. The gathering of ambient energy by a harvester and transferring it to storage units in the form of an electrical energy method has been shown and all the benefits have been discussed as well as drawbacks. For example, some of harvester devices are not efficient enough, such as solar, which requires a bigger solar cell area to gain energy, or thermal, which demands a temperature difference, which can be a problem in small-scaled devices. Also the general principles of operation of the whole system of Energy Harvester Device, Wireless Sensor Networks and MCU/controller have been summarized and reviewed.

The selection of the proper harvester device is dependent on many aspects. For example, place of operation, scale of the project, or the type of implemented mechanism. Obviously each harvester has its own pros, but main aim of this thesis is to research the

Piezoelectric Energy Harvesting Device. Mostly in development of Analytical Method it has been relied on S. Roundy and P. K. Wright [34]. A mathematical model has been derived and a computational analytical model has been simulated. Wireless Sensors operate at low power, approximately 200 μW which has been reached in the first design, and it was compared to experiments provided by S. Roundy. Unfortunately, experiments conducted during this thesis were not available due to some other reasons. The main factors that should be followed while designing a Piezoelectric Energy Harvester are that PEHs operate approximately at their resonance frequency, and to reach their highest power output, they should operate at the value of their driven frequency. In Equation (3.47) it is shown that $\omega_n = \omega$ and all the following device designs have been constructed according to this factor.

Finally for the future designs and optimization of the PEHs other details have been reviewed. To sum up it is better to have shorter beam if it is important to achieve high Power and Voltage. Width of a beam does not much affect on a Voltage, however it proportional to the output power. Beam thickness ratio does not act on Power, but it influence on the Voltage and Current being proportional to Voltage and Inverse proportional to Current. Last thing to mention in design of a cantilever beam Piezoelctric Energy Harvesting Device is mass. The proof mass linked to the system determines the power output. As a result, the proof mass should be maximized while other limitations like resonance frequency and strain limits are respected. For that reason for the first design operation frequency range has been found and optimal frequency has been selected 204.6158 Hz, and this was implemented for further device designs.

For the future work, I hope to continue this research and do all the experiments needed to see for myself the errors in computational results. Unfortunately, I could not get results from Finite Element Analysis of a beam. This is why, in the future, I would like to provide a full numerical simulation and analysis of the system. Provide experiments with harvesters collaborating with different storage units, most likely capacitors, as this new field is less explored and more promising. A further plan is to obtain an optimal design of a Piezoelectric Energy Harvesting Device that can replace batteries for Wireless Sensor Networks.

Bibliography

[1] SP Beeby, MJ Tudor, E Koukharenko, NM White, T O'Donnell, C Saha, S Kulkarni, and S Roy. Design, fabrication and simulations of microelectromagnetic vibration powered generator for low power mems. 2005.

[2] Haluk Kulah and Khalil Najafi. An electromagnetic micro power generator for low-frequency environmental vibrations. In *17th IEEE International Conference on Micro Electro Mechanical Systems. Maastricht MEMS 2004 Technical Digest*, pages 237–240. IEEE, 2004.

[3] Shad Roundy, Eli S Leland, Jessy Baker, Eric Carleton, Elizabeth Reilly, Elaine Lai, Brian Otis, Jan M Rabaey, Paul K Wright, and V Sundararajan. Improving power output for vibration-based energy scavengers. *IEEE Pervasive computing*, 4(1):28–36, 2005.

[4] CB Williams and Rob B Yates. Analysis of a micro-electric generator for microsystems. *sensors and actuators A: Physical*, 52(1-3):8–11, 1996.

[5] Ghislain Despesse, Thomas Jager, Jean-Jacques Chaillout, Jean-Michel Léger, and Skandar Basrour. Design and fabrication of a new system for vibration energy harvesting. *Research in microelectronics and electronics*, 1:225–228, 2005.

[6] Shad Roundy, Paul K Wright, and Kristofer SJ Pister. Micro-electrostatic vibration-to-electricity converters. In *ASME international mechanical engineering congress and exposition*, volume 36428, pages 487–496, 2002.

[7] EA Skow, KA Cunefare, and A Erturk. Power performance improvements for high pressure ripple energy harvesting. *Smart materials and structures*, 23(10):104011, 2014.

[8] Kenneth A Cunefare, EA Skow, Alper Erturk, J Savor, N Verma, and MR Cacan. Energy harvesting from hydraulic pressure fluctuations. *Smart Materials and Structures*, 22(2):025036, 2013.

[9] Wendi Rabiner Heinzelman, Anantha Chandrakasan, and Hari Balakrishnan. Energy-efficient communication protocol for wireless microsensor networks. In *Proceedings of the 33rd annual Hawaii international conference on system sciences*, pages 10–pp. IEEE, 2000.

[10] Saurabh Ganeriwal, Deepak Ganesan, Hohyun Shim, Mani Srivastava, and Mark Hansen. Sys4: Estimating clock uncertainty for efficient duty-cycling in sensor networks. 2005.

[11] Omprakash Gnawali, Ki-Young Jang, Jeongyeup Paek, Marcos Vieira, Ramesh Govindan, Ben Greenstein, August Joki, Deborah Estrin, and Eddie Kohler. The tenet architecture for tiered sensor networks. In *Proceedings of the 4th international conference on Embedded networked sensor systems*, pages 153–166, 2006.

[12] Xiaorui Wang, Guoliang Xing, Yuanfang Zhang, Chenyang Lu, Robert Pless, and Christopher Gill. Integrated coverage and connectivity configuration in wireless sensor networks. In *Proceedings of the 1st international conference on Embedded networked sensor systems*, pages 28–39, 2003.

[13] Sujesha Sudevalayam and Purushottam Kulkarni. Energy harvesting sensor nodes: Survey and implications. *IEEE communications surveys & tutorials*, 13(3):443–461, 2010.

[14] Xiaofan Jiang, Joseph Polastre, and David Culler. Perpetual environmentally powered sensor networks. In *IPSN 2005. Fourth International Symposium on Information Processing in Sensor Networks, 2005.*, pages 463–468. IEEE, 2005.

[15] Chris Knight, Joshua Davidson, and Sam Behrens. Energy options for wireless sensor nodes. *Sensors*, 8(12):8037–8066, 2008.

[16] Shad Roundy, Paul Kenneth Wright, and Jan M Rabaey. Energy scavenging for wireless sensor networks. In *Norwell*, pages 45–47. Springer, 2003.

[17] Josh Davidson. *Energy harvesting for marine based sensors.* PhD thesis, James Cook University, 2016.

[18] D Halliday, R Resnick, and J Walker. Fundamentals of physics (vol. 1, pp. 93–105), 2008.

[19] Yongjia Wu. *Thermoelectric Energy Harvesting for Sensor Powering.* PhD thesis, Virginia Tech, 2019.

[20] Maryam Hamlehdar, Alibakhsh Kasaeian, and Mohammad Reza Safaei. Energy harvesting from fluid flow using piezoelectrics: A critical review. *Renewable Energy*, 143:1826–1838, 2019.

[21] Abdessattar Abdelkefi. Aeroelastic energy harvesting: A review. *International Journal of Engineering Science*, 100:112–135, 2016.

[22] Shashank Priya and Daniel J Inman. *Energy harvesting technologies*, volume 21. Springer, 2009.

[23] Scott Meninger, Jose Oscar Mur-Miranda, Rajeevan Amirtharajah, Anantha Chandrakasan, and Jeffrey H Lang. Vibration-to-electric energy conversion. *IEEE Transactions on Very Large Scale Integration (VLSI) Systems*, 9(1):64–76, 2001.

[24] Shad Roundy, Paul K Wright, and Jan Rabaey. A study of low level vibrations as a power source for wireless sensor nodes. *Computer communications*, 26(11):1131–1144, 2003.

[25] Hiroyuki Nishide and Kenichi Oyaizu. Toward flexible batteries. *Science*, 319(5864):737–738, 2008.

[26] Anthony G Pandolfo and Anthony F Hollenkamp. Carbon properties and their role in supercapacitors. *Journal of power sources*, 157(1):11–27, 2006.

[27] Jurgen Garche, Chris K Dyer, Patrick T Moseley, Zempachi Ogumi, David AJ Rand, and Bruno Scrosati. *Encyclopedia of electrochemical power sources*. Newnes, 2013.

[28] Ryan W Hart, Henry S White, Bruce Dunn, and Debra R Rolison. 3-d microbatteries. *Electrochemistry communications*, 5(2):120–123, 2003.

[29] Pramod Kumar Sharma and Prashant V Baredar. Analysis on piezoelectric energy harvesting small scale device–a review. *Journal of King Saud University-Science*, 31(4):869–877, 2019.

[30] SM Taware and SP Deshmukh. A review of energy harvesting from piezoelectric materials. *IOSR Journal of Mechanical and Civil Engineering (IOSR-JMCE)*, pages 43–50, 2013.

[31] Ashok K Batra, Almuatasim Alomari, Ashwith K Chilvery, Alak Bandyopadhyay, and Kunal Grover. Piezoelectric power harvesting devices: an overview. *Advanced Science, Engineering and Medicine*, 8(1):1–12, 2016.

[32] Meiling Zhu, Emma Worthington, and Ashutosh Tiwari. Design study of piezoelectric energy-harvesting devices for generation of higher electrical power using a coupled piezoelectric-circuit finite element method. *IEEE transactions on ultrasonics, ferroelectrics, and frequency control*, 57(2):427–437, 2010.

[33] Renato Caliò, Udaya Bhaskar Rongala, Domenico Camboni, Mario Milazzo, Cesare Stefanini, Gianluca De Petris, and Calogero Maria Oddo. Piezoelectric energy harvesting solutions. *Sensors*, 14(3):4755–4790, 2014.

[34] Shad Roundy and Paul K Wright. A piezoelectric vibration based generator for wireless electronics. *Smart Materials and structures*, 13(5):1131, 2004.

[35] Anita M Flynn and Seth R Sanders. Fundamental limits on energy transfer and circuit considerations for piezoelectric transformers. *IEEE transactions on power electronics*, 17(1):8–14, 2002.

[36] Ferdinand P Beer, ER Johnston, JT DeWolf, and DF Mazurek. Mechanics of materials. *New York*, 1992.

[37] Jan M Rabaey, Josie Ammer, Tufan Karalar, Suetfei Li, Brian Otis, Mike Sheets, and Tim Tuan. Picoradios for wireless sensor networks: the next challenge in ultra-low power design. In *2002 IEEE International Solid-State Circuits Conference. Digest of Technical Papers (Cat. No. 02CH37315)*, volume 1, pages 200–201. IEEE, 2002.

[38] S P Beeby, M J Tudor, and NM White. Energy harvesting vibration sources for microsystems applications. *Measurement science and technology*, 17(12):R175, 2006.

[39] William T Thomson. *Theory of vibration with applications*. CrC Press, 2018.

[40] D-G Lee, GP Carman, D Murphy, and C Schulenburg. Novel micro vibration energy harvesting device using frequency up conversion. In *TRANSDUCERS 2007-2007 International Solid-State Sensors, Actuators and Microsystems Conference*, pages 871–874. IEEE, 2007.

[41] Vinod R Challa, MG Prasad, Yong Shi, and Frank T Fisher. A vibration energy harvesting device with bidirectional resonance frequency tunability. *Smart Materials and Structures*, 17(1):015035, 2008.

[42] Gregory J Pottie. Wireless sensor networks. In *1998 Information Theory Workshop (Cat. No. 98EX131)*, pages 139–140. IEEE, 1998.

[43] Shad Roundy, Brian P Otis, Yuen-Hui Chee, Jan M Rabaey, and Paul Wright. A 1.9 ghz rf transmit beacon using environmentally scavenged energy. *optimization*, 4(2):4, 2003.

[44] George A Lesieutre, H Hofmann, and G Ottmann. Structural damping due to piezoelectric energy harvesting. In *13th International Conference on Adaptive Structures and Technologies*, pages 368–377, 2004.

[45] P Glynne-Jones, SP Beeby, EP James, and NM White. The modelling of a piezoelectric vibration powered generator for microsystems. In *Transducers' 01 Eurosensors XV*, pages 46–49. Springer, 2001.

[46] Salem Saadon and Othman Sidek. A review of vibration-based mems piezoelectric energy harvesters. *Energy conversion and management*, 52(1):500–504, 2011.

[47] Geffrey K Ottman, Heath F Hofmann, Archin C Bhatt, and George A Lesieutre. Adaptive piezoelectric energy harvesting circuit for wireless remote power supply. *IEEE Transactions on power electronics*, 17(5):669–676, 2002.

[48] Thomas von Büren and Gerhard Tröster. Design and optimization of a linear vibration-driven electromagnetic micro-power generator. *Sensors and Actuators A: Physical*, 135(2):765–775, 2007.

[49] Conrad Donovan, Alim Dewan, Huan Peng, Deukhyoun Heo, and Haluk Beyenal. Power management system for a 2.5 w remote sensor powered by a sediment microbial fuel cell. *Journal of Power Sources*, 196(3):1171–1177, 2011.

[50] Nathan S Shenck and Joseph A Paradiso. Energy scavenging with shoe-mounted piezoelectrics. *IEEE micro*, 21(3):30–42, 2001.

[51] Subhas Chandra Mukhopadhyay and Henry Leung. *Advances in wireless sensors and sensor networks*, volume 64. Springer, 2010.

[52] Jun Zheng and Abbas Jamalipour. *Wireless sensor networks: a networking perspective*. John Wiley & Sons, 2009.

[53] Borja Pozo, José Ignacio Garate, José Ángel Araujo, and Susana Ferreiro. Energy harvesting technologies and equivalent electronic structural models. *Electronics*, 8(5):486, 2019.

[54] Pavlos Papageorgiou. Literature survey on wireless sensor networks, 2003.

[55] Kawa Haji Mahmoud. Data collection and processing from distributed system of wireless sensors. *Masaryk University, Thesis*, 2013.

[56] Giacomo Ferrarese and Stefano Malavasi. *Energy harvesting: Technology, methods and applications*. Renee Williams, 2015.